Biofilm formation strongly influences the vector transport of triclosan-loaded polyethylene microplastics

Irene Verdú, Georgiana Amariei, Cristina Rueda-Varela, Miguel González-Pleiter, Francisco Leganés, Roberto Rosal, Francisca Fernández-Piñas. Biofilm formation strongly influences the vector transport of triclosan-loaded polyethylene microplastics. Science of The Total Environment 859, Part 1, 160231, 2023.

https://doi.org/10.1016/j.scitotenv.2022.160231

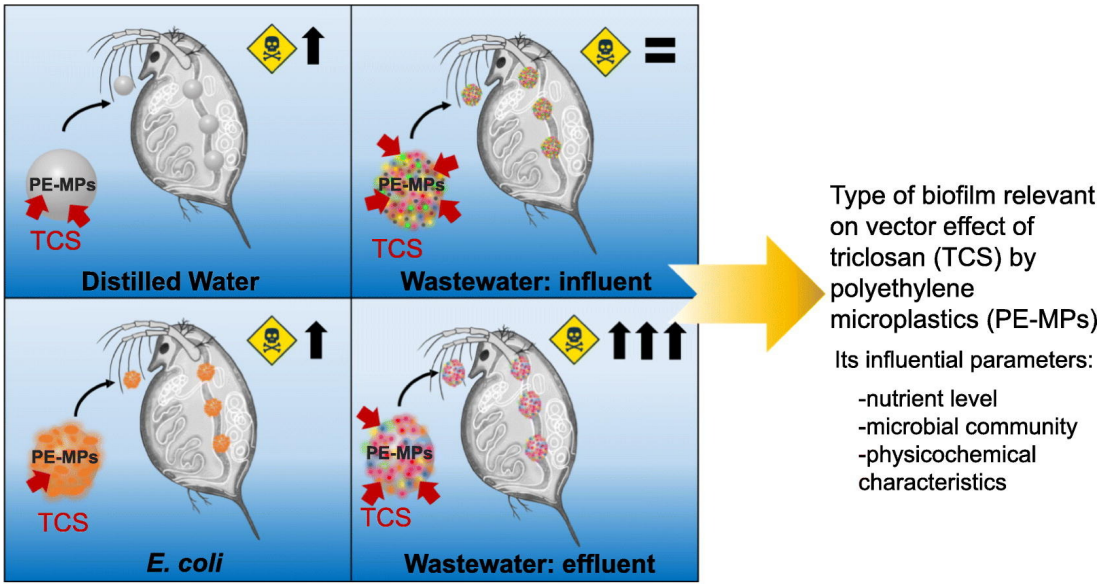

Biofilm formation strongly influences the vector transport of triclosan-loaded polyethylene microplastics

Irene Verdú[1], Georgiana Amariei[2], Cristina Rueda-Varela[1], Miguel González-Pleiter[1], Francisco Leganés[1,3], Roberto Rosal[2], Francisca Fernández-Piñas[1,*]

[1]Department of Biology, Faculty of Science, Universidad Autónoma de Madrid, E-28049 Madrid, Spain
[2]Department of Chemical Engineering, Universidad de Alcalá, E-28871, Alcalá de Henares, Madrid, Spain
[3]Centro de Investigación en Biodiversidad y Cambio Global, Universidad Autónoma de Madrid. Darwin 2, 28049 Madrid, Spain

Abstract

This study aimed at evaluating the influence of biofilm in the role of microplastics (MPs) as vectors of pollutants and their impact on *Daphnia magna*. To do this, virgin polyethylene MPs, (PE-MPs, 40–48 µm) were exposed for four weeks to wastewater (WW) from influent and effluent to promote biofouling. Then, the exposed PE-MPs were put in contact with triclosan. Finally, the toxicity of TCS-loaded and non-TCS loaded PE-MPs were tested on the survival of *D. magna* adults for 21 days. Results from metabarcoding analyses indicated that exposure to TCS induced shifts in the bacterial community, selecting potential TCS-degrading bacteria. Results also showed that PE-MPs were ingested by daphnids. The most toxic virgin PE-MPs were those biofouled in the WW effluent. The toxicity of TCS-loaded PE-MPs biofouled in the WW effluent was even higher, reporting mortality in all tested concentrations. These results indicate that biofouling of MPs may modulate the adsorption and subsequent desorption of co-occurring pollutants, hence affecting their potential toxicity towards aquatic organisms. Future studies on realistic environmental plastic impact should include the characterization of biofilms growing on plastic. Since inevitably plastic biofouling occurs over time in nature, it should be taken into account as it may modulate the sorption of co-occurring pollutants.

1. Introduction

Plastic pollution is an emerging concern and a new field of research. Plastic production has constantly increased from 2 million tons in 1950 to 367 million tons in 2020, but its recovery rate is still scarce (PlasticsEurope, 2021; OECD, 2022). It has been estimated that 53 million tons of plastic waste will be annually discharged into aquatic ecosystems by 2030 (Geyer et al., 2017; Borrelle Stephanie et al., 2020; Geyer, 2020; PlasticsEurope, 2021; OECD, 2022). The smallest fractions such as microplastics (MPs), understood as plastic particles < 5 mm in their largest dimension, represent a widespread contaminant in terrestrial and aquatic ecosystems. Despite the high removal capacity of wastewater treatment plants (WWTPs) for MPs, a large amount of them ends up in the rivers and other water bodies due to their continued release from treated sewage. The small size, density, and persistence of MPs make them highly mobile allowing them to reach a variety of ecosystems through WWTPs discharges (Murphy et al., 2016; Ziajahromi et al., 2016; Kay et al., 2018). In fact, the emissions from WWTPs are considered the mainland-based way of entry of MPs into freshwater environments (Ziajahromi et al., 2017). Once released into aquatic systems, MPs can be transported to the oceans through rivers, but a significant part accumulates in inland reservoirs, such as sediments or lakes (Browne et al., 2011; Free et al., 2014). The data available for freshwater environments show concentrations reaching a few grams per liter of water in rivers and lakes, and typically higher concentrations in sediments. In most cases, polyethylene (PE) is the most reported polymer (Li et al., 2018; Li et al., 2020; Yang et al., 2021).

MPs have been associated with a broad range of hazards for freshwater wildlife including physical irritation, blockage of gills and digestive tract, mortality, oxidative stress, antioxidant activity, cytotoxicity, or genotoxicity (Lambert and Wagner, 2018). In recent years considerable attention has been paid to the possible role of MPs as vectors of other chemical compounds found in the environment, such as pharmaceuticals and personal care products, heavy metals, flame retardants, plasticizers, or hydrophobic organic contaminants (Wu et al., 2016; Jemec Kokalj et al., 2019; González-Pleiter et al., 2021; Verdú et al., 2021). Through interaction with MPs, the bioavail-

* Corresponding author: francisca.pina@uam.es,
Available online: November 17, 2022

ability of sorbed pollutants could increase due to the ingestion of pollutant-loaded particles and subsequent desorption in the digestive system, or by pollutant transfer to the aqueous phase or to food sources potentially inducing increased exposure for certain organisms (Browne et al., 2013; Hartmann et al., 2017). Pollutant transfer potential by plastics has been shown to depend on polymer properties such as size, morphology, density, crystallinity, and chemical composition, pollutant characteristics like hydrophobicity and charge, and the properties of the receiving media, such as temperature, salinity, pH, or exposure to solar radiation. Upon aging, polymer properties can be modified, thereby influencing the behavior of MPs and their interaction with pollutants (Cole et al., 2011; Andrady, 2017; Lambert et al., 2017).

MPs can be rapidly colonized by microorganisms (Salta et al., 2013; Zettler et al., 2013; Amaral-Zettler et al., 2015; Miao et al., 2019). The plastisphere, a term usually used to denote the microbial community that colonizes plastics (biofilm attached to the plastic), consists of a great variety of microorganisms including heterotrophs, autotrophs, predators, and symbionts (Zettler et al., 2013; Amaral-Zettler et al., 2020). These microorganisms structure themselves into sessile communities embedded by an extracellular matrix whose taxonomic composition differs from that of the surrounding medium or from that established on other substrates (Zettler et al., 2013; Rummel et al., 2017). It has been shown that microbial diversity in biofilms developed on plastics depends on environmental conditions such as temperature, salinity, pressure, light, and oxygen concentration, and, to a lesser extent, on the type and properties of the plastic itself (Jacquin et al., 2019; Martínez-Campos et al., 2021). Interestingly, several authors have observed that biofouling could increase MPs ingestion by filtering organisms due to the emission of attracting chemical signals (Savoca et al., 2016; Savoca et al., 2017; Vroom et al., 2017; Horváthová and Bauchinger, 2019; Zimmermann et al., 2020; Tang et al., 2021; Amariei et al., 2022).

The presence of a wide range of functional groups in biofilms and the fact that they may contain pollutant-degrading microorganisms could affect the sorption, desorption, and fate of the chemicals interacting with MPs, thereby altering their role as pollutant carriers (Lobelle and Cunliffe, 2011; Carson, 2013; Eerkes-Medrano et al., 2015; Hartmann et al., 2017; Guan et al., 2020; Tu et al., 2020; Wang et al., 2020).To date, most available data on the vector transport of pollutants by plastics have been obtained from experiments with pristine MPs, but the characteristics of environmentally aged materials may lead to significantly different interactions with chemicals (Phuong et al., 2016; de Sá et al., 2018). At present, the body of knowledge on the influence of biofilm formation on the role of MPs as vectors of pollutants is still very scarce. Guan et al. (2020) and Wu et al. (2022) found an increase in the sorption capacity of biofouled polystyrene for some metals (Cd, Cr, Ni, Zn, Cu, Co, and Ag) compared to non-biofouled specimens. Wang et al. (2020) also reported higher sorption of copper and tetracycline by biofouled PE. Similar results have been found elsewhere for different polymers and pollutants (Richard et al., 2019; Qi et al., 2021). Concerning the biological impact of biofouled MPs, Qi et al. (2021) showed that the toxicity of lead to *D. magna* increased for biofouled PS compared to virgin material. Because the fate of MPs in actual environmental scenarios is largely governed by their interactions with living organisms, further research is required to fully understand the role of biofilms developed on MPs in the transfer of pollutants to the biota and their potential risks (Wang et al., 2021).

To the best of our knowledge, this is the first work studying the influence of biofilm formation on PE-MPs biofouled in environmental matrices on the role of MPs as vectors of emerging contaminants. For that purpose, we chose triclosan (TCS), a biocide found in many consumer goods, which is only partially removed in conventional WWTPs, PE was selected as it is one of the most abundant plastic pollutants. Treated and untreated wastewater were used as matrices for PE-MPs biofouling, because, as outlined before, it is the main source of entry of pollutants and MPs into the aquatic environments (Browne et al., 2011; Chen et al., 2011; Li et al., 2020). *Daphnia magna* was chosen as the model organism due to its importance in ecotoxicology as a non-selective filter-feeder and its role as a primary consumer in the food web in freshwater ecosystems. For that purpose, biofilms were allowed to grow on MPs incubated in treated (effluent) and untreated (influent) wastewater and their sorption-desorption capacity for TCS was evaluated. The impact of TCS-loaded PE-MPs both pristine and biofouled on *D. magna* survival was studied. Metabarcoding analyses were also performed to study the microbial community composition in the biofilms attached to the PE-MPs both in the presence and absence of TCS.

2. Materials and methods

2.1 Materials and reagents

Commercial PE-MPs (PE, 40–48 μm, density 0.94 g/mL, irregular shaped fragments) were purchased from Sigma-Aldrich (CAS number 9002-88-4). Prior

to use, PE-MPs were washed with methanol (100 %) and several times with distilled water to ensure the removal of any sorbed material. Subsequently, they were dried in glass beakers at 50 °C overnight. Finally, they were sieved through a 10 µm pore size sieve to remove small particles. A stock suspension (36,700 mg/L) was prepared in distilled water, briefly sonicated, and stored at 4 °C in a glass flask until use. The experimental Fourier-transform infrared (FTIR) spectra, the morphology, and size distribution of PE-MPs were assessed using a ThermoScientific Nicolet iS10 apparatus with a Smart iTR-Diamond module, an Olympus CX41 microscope with digital color camera Olympus DP20 and a Beckman-coulter Z2 particle size analyzer, respectively (Fig. S1, Supplementary Material, SM).

Triclosan (TCS) (5-Chloro-2-(2,4-dichlorophenoxy) phenol, TCS, C12H7Cl3O2, CAS number: 3380-34-5, purity $\geq$ 97.0 %) was purchased from Sigma-Aldrich. A stock solution (10,000 mg/L) was prepared in MeOH (100 %), because of the low solubility of TCS in water (10 mg/L). The stock was stored at 4 °C in amber glass flasks until use.

2.2 PE-MPs biofouling procedure

PE-MPs were allowed to be colonized in wastewater to promote biofouling. As negative colonization control, sterile distilled water (hereinafter DW) was used in the biofouling experiment; as positive colonization control, Escherichia coli (*Escherichia coli*) cultures (Ec) grown in LB (Luria-Bertani) medium with an initial concentration of 10^6 cells/mL were also used in the biofouling experiment. Water samples were collected from the primary (influent) and secondary (effluent) clarifiers of a wastewater treatment plant (WWTP) close to Madrid designed to treat 45,000 m^3/day of urban wastewater. Wastewater samples were immediately transported to the laboratory to start the biofouling experiments. Hereinafter wastewater samples will be referred to as influent (INF) and effluent (EFL), respectively. Prior to colonization experiments, 2 L of each wastewater and controls were mixed with 10 mL of PE-MPs and sonicated for 30 s. The PE-MPs concentration was 183.5 mg MPs/L (1.57×10^7 particles/L); this concentration is slightly below that estimated for freshwaters which can range up to 10^8 particles/L as reported by Koelmans et al. (2019). The incubation experiments were carried out in glass bottles and three replicates were conducted for each type of water. Samples were kept at 25 °C using a photoperiod of 16 h of light and 8 h of dark and manually shaken twice per day for 4 weeks (Guan et al., 2020). After the prescribed colonization time, a pressure holder (Millipore) with a nylon mesh filter (47 mm, 10 µm of pore size) was used to filter the resulting material. The obtained PE-MPs, namely PE-MPs in DW (MPs-DW); Ec (MPs-Ec); influent (MPs-INF), and effluent (MPs-EFL), were recovered and dispersed in distilled water with a final mass concentration of 10.0 g/L to be used as stocks as explained below. Water samples taken before and after colonization experiments were stored at -20 °C for further metabarcoding and chemical analyses.

2.3 TCS sorption and desorption experiments

Biofouled PE-MPs stocks were briefly sonicated (5 s) prior to TCS exposure. For it, 1 mg/L of TCS was put in contact with 10,000 mg/L of PE-MPs for 4 h in glass flasks (pH 6.5). Samples were incubated in a rotary shaker (50 rpm) at room temperature and in darkness to prevent photodegradation. After the prescribed time, MPs were recovered by filtration (nylon mesh filter with 10 µm pore size), obtaining TCS-loaded PE-MPs (tMPs). To determine the amount of TCS sorbed by the differently biofouled PE-MPs, 0.05 g (plastics dry weight determined as explained below) of each material was extracted by sonication in pure acetonitrile (ACN) for 2 h (HPLC grade, Sigma-Aldrich). The dry weight of plastics was determined by treating the samples of biofouled plastics with H_2O_2 (33 %) for 24 h with the aim of removing the microorganisms and all the remains of organic matter adhered during biofouling. In addition to sorption, the desorption of TCS from MPs was assessed in the culture medium used for bioassays (see below) after 0, 1, 4, 7, 10, 14, 18, and 21 days following the exposure of PE-MPs to TCS. TCS concentration in ACN extracts and in culture media was measured by high-performance liquid chromatography (HPLC), using a 1200 Series Agilent Technologies apparatus equipped with Promosil C18 (5 µm, 100 Å, 4.6 × 150 mm) column and using a diode array detector. The mobile phase was 70:30, v v-1 ACN: Milli-Q water adjusted to pH 2 with H_3PO_4. The flow rate was 1 mL/min and the injection volume was 20 µL. A preconcentration technique (solid phase extraction) was used when necessary (Strata-X 33u Polymeric Reversed Phase cartridges, Phenomenex). The amount of TCS sorbed was expressed as µg TCS/g PE-MP for sorption and µg TCS/mL for desorption.

2.4. Biofilm characterization and metabarcoding analyses

Confocal fluorescence microscopy (Leica Microsystems Confocal, SP5 Fluorescence microscope, Germany) was used to assess biofilm formation during biofouling experiments and to check whether TCS

exposure affected the presence and viability of microorganisms. For it, non-exposed PE-MPs and tMPs were incubated with different fluorochromes after sonication for 10 s to disperse possible aggregates. PE-MPs were stained with FilmTracer™ SYPRO Ruby Biofilm Matrix Stain (Thermo Fisher Scientific) to assess the presence of proteins in the biofilm matrix. Film Tracer FM 1-43 Green Biofilm Cell Stain (Thermo Fisher Scientific), was used to stain cell bodies and Live/Dead BacLight Bacterial Viability kit (Thermo Fischer Scientific) to assess the bacterial viability in the biofilm according to the manufacturer's instructions.

The bacterial community composition of biofouled MPs and tMPs (MPs-INF, MPs-EFL, tMPs-INF, and tMPs-EFL) was characterized by paired-end Illumina MiSeq 2 × 300 system sequencing of 16 s rRNA. In addition, the bacterial community composition from surrounding waters (INF and EFL) at the beginning (INF-t0 and EFL-t0) and at the end of the biofouling experiments (INF-t4 and EFL-t4) was also characterized. For that, samples from each PE-MPs type and wastewater samples were previously filtered by 0.22 µm nylon filters and stored at -20 °C prior to DNA extraction. A detailed protocol is given in SM as Supplementary Text 1.

Sequences used in this study were submitted to the National Center for Biotechnology Information (http://www.ncbi.nlm.nih.gov/) under the Bioproject accession number: PRJNA884487.

2.5. Characterization of water samples and PE-MPs

The physicochemical properties of water were measured before and after biofouling: pH (Crison pH 25+) conductivity (µS/cm, Crison MM 40++); dissolved O_2 (mg/L, Crison OXI 45+); absorbance at 600 nm and 260 nm, which inform about the presence of bacteria and exopolysaccharides (UV 1800 Shimazu spectrophotometer) (Stevenson et al., 2016; Trabelsi et al., 2009); dissolved and suspended non-purgeable total organic carbon (NPOC) (mg/L, Total Organic Carbon Analyzer TOC-VCAH, Shimadzu) and ions, quantified by ion chromatography (Metrohm 930 Compact IC Flex apparatus) are shown in Tables S2 and S3 (SM). All analyses were run in triplicate.

Infrared spectra of PE-MPs were obtained by means of Attenuated Total Reflectance Fournier Transform spectroscopy (ATR-FTIR). For that, a Thermo Scientific Nicolet iS10 apparatus with a Smart iTR-Diamond module and OMNIC 8.3 software was used in the 4000–600 cm^{-1} range with a resolution of 4 cm^{-1} and 32 scans. MPs size particle distribution prior to and after TCS exposure was determined using a Coulter Particle Counter and size analyzer Z2 (Beckman Coulter Inc., Miami, USA) equipped with a 100 µm aperture. Hydrophobicity was determined by means of optical contact angle (Krüss DSA25Drop Shape Analysis System) at room temperature, using distilled water drops. Likewise, the concentration of total proteins, lipids, and carbohydrates was measured, using 20 mg of each PE-MP following the methodology described by De Coen and Janssen (1997) and modified by Rodrigues et al. (2015). A microplate reader (Synergy HT multimode microplate reader, BioTek, Seattle, WA) was used for absorbance measurements and the results were expressed as mg/g of PE-MP. Total reflection X-ray Fluorescence (TXRF S2 PicoFox, Bruker), was used to determine some microelements present in MPs-INF and MPs-EFL.

2.6. Bioassays

Daphnia magna ecotoxicity tests were conducted according to OECD 211 (OECD, 2012), with minor modifications as explained elsewhere (Amariei et al., 2022). The commercial kit DaphtoxkitF magna (Creasel, Belgium), was used to obtain the specimens. To induce hatching, dormant eggs were incubated in Standard Freshwater medium (FW) at pH 7.2 at 22 °C under continuous illumination (6000 lx). *D. magna* organisms (20 individuals) were maintained in 1 L-glass beakers with 800 mL of previously aerated culture medium. The daphnids were fed with the green microalgae *Chlamydomonas reinhardtii* obtained from a running culture.

In Fig. S1 (SM) a diagram of the experimental design is depicted. Adult individuals, 10-days old, were exposed to 0, 25, 50, 100, 200 and 400 mg/L (2.13×10^6, 4.27×10^6, 8.54×10^6, 1.71×10^7, and 3.42×10^7 particles/L respectively) of PE-MPs kept 4 weeks in DW, Ec, INF and EFL, namely MPs-DW, MPs-Ec, MPs-INF, and MPs-EFL, respectively, in test tubes with 20 mL of FW medium adjusted to pH 7.2. The same concentrations were used for TCS-loaded PE-MPs (tMPs). Non-exposed organisms in FW medium were used as controls. Each treatment exposed 15 individuals (Three replicates with five organisms each), and six replicates with five organisms each were run for controls (30 individuals). The green microalgae *Chlamydomonas reinhardtii* at a concentration of 0.2 mg organic carbon/L was used every 2 days for *D. magna* feeding, which was above the limiting food concentration (Ogonowski et al., 2016). The tubes were incubated at 22 °C and 16/8 photoperiod in a laboratory chamber. The test was run for 21 days, during which samples were daily shaken, and survival evaluated. *D. magna* specimens were considered dead when no movement was registered for 15 s after gentle shaking. At the end of expo-

sure time, organisms were collected and observed, using microscopy (Olympus CX41 microscope with digital color camera Olympus DP20 or stereo microscope Motic SMZ 140 Series) in order to visualize the presence of PE-MPs in their digestive tract.

2.7. Statistical analysis

Time-to-event data analysis was used to evaluate the toxicity on *D. magna* survival for the different treatments tested throughout the whole experimental period (21 d) (Hosmer et al., 2008). Kaplan Meier curves were used to represent the survival of specimens (Kelpsiene et al., 2020). Median lethal times (LT_{50}) were also determined. Then, log-rank tests were run to analyze statistically significant differences between pairwise survival curves. In TCS sorption experiments, one-way analysis of variance (ANOVA) and post-hoc Tukey's HSD tests, were performed after having checked the assumptions required for parametric analysis, in order to determine the statistical differences between the TCS concentration sorbed in each type of PE-tMPs (tMPs-DW, tMPs-Ec, tMPs-INF, and tMPs-EFL). A p-value of $p < 0.05$ was used to assess significant differences. Statistical computing software GraphPad Prism 8.0.2 was used to do the aforementioned analyses.

2.8. Quality assurance/quality control assessment

Quality Assurance/Quality Control assessment (QA/QC) followed de Ruijter et al. (2020). QA/QC evaluation scores are provided in Table S4 (SM).

3. Results and discussion

The formation of biofilm was assessed along the four-week colonization assays. As expected, no evidence of biofilm formation was observed in MPs-DW, which served as negative biofouling control (Fig. S3, Fig. S4, SM). However, in MPs-Ec, MPs-INF, and MPs-EFL the presence of biofilm was clear. In the FTIR spectrum, presented in Fig. S5, the appearance of new peaks and altered regions could be attributed to biofouling. So, the presence of EPS proteins (amide I, 1600–1700 cm^{-1}; amide II, 1500–1600 cm^{-1}; amide II, 1200–1350 cm^{-1}), polysaccharides (900–1500 cm^{-1}), and lipids (2800–2970 cm^{-1}) were detected (Mosharaf et al., 2018). Moreover, micrographs in Figs. S3 showed the presence of biofilm with most cells showing to be viable in MPs-INF and MPs-EFL, as well as in the positive colonization control (MPs-Ec). After the exposure to TCS, the micrographs generally showed a high cell density with most cells in a viable state, as well as detectable levels of EPS, so the data suggested that the 4 h exposure to TCS did not affect cell survival (Fig. S4).

The bacterial community composition of the biofilm formed on PE-MPs (MPs-INF and MPs-EFL) and PE-tMPs (tMPs-INF and tMPs-EFL) and water samples (INF-t0, INF-t4, EFL-t0, and EFL-t4) was characterized. 2,888,624 reads corresponding to the 16S rRNA gene were obtained using Illumina sequencing. After filtering and trimming the reads, merging, and removal of possible chimeras, 1,610,930 high-quality reads remained. Based on 99 % sequence similarity, these reads were clustered into 1718 ASVs (Amplicon Sequence Variants) for bacteria. The rarefaction curves for all samples approached the saturation plateau, pointing out that the libraries were adequately sampled (Fig. S6, SM). Bacterial α-diversity was estimated using the Shannon Index (Fig. 1A). The values of the Shannon index did not show significant differences between influent samples (MPs-INF and influent water samples), but a significant higher α-diversity was obtained for MPs-EFL and tMPs-EFL with respect to the effluent wastewater samples (EFL-t0 and EFL-t4) ($p < 0.05$) (Fig. 1A). This lower diversity in free-living bacteria in the effluent water in comparison to those attached to MPs was already reported by McCormick et al., (2014) and Martínez-Campos et al. (2021). Likewise, there were no differences in α-diversity between biofilm bacterial communities attached to MPs previously exposed or non-exposed to TCS (MPs-INF, tMPs-INF, MPs-EFL, and tMPs-EFL). However, β-diversity (PCoA plot) revealed a clear clustering pattern of MPs and tMPs. The first PCoA component explained 17.5 % of the difference between clusters, and the second 15.3 % (Fig. 1B). PERMANOVA analysis (Table S5, SM) revealed significant differences between the analyzed factors ($p < 0.05$), being TCS exposure and the interaction Substrate x WW x TCS, which mostly explained the observed variability (higher R^2).

Taxonomic analysis showed that the majority of the ASVs were associated with the phylum Proteobacteria, which is the most abundant phyla in all the treatments (33–89 %), followed by Bacteroidota (4–18 %) (Fig. 2). However, the next most abundant phyla varied depending on the type of sample, Firmicutes dominating in INF-t0; Actinobacteria in INF-t4; Nitrospirota in MPs-INF; Actinobacteriota in tMPs-INF; Patescibacteria in EFL-t0; Cyanobacteria in EFL-t4; Planctomycetota and Acidobacteriota in MPs-EFL; and finally, Chlorofelxi in tMPs-EFL. The most abundant taxa in each plastic sample are shown in Table S6, SM, MPs-INF biofilm was characterized by a high abundance (≥ 1 %) of taxa such as Nitrospira (15.3 ± 1.1 %), Dokdonella (7.9 ± 0.3 %)

and Arenimonas (6.3 ± 1.0 %), genera related to the nitrogen and carbon biochemical cycles. In MPs-EFL, these genera were not present, or the relative abundance was much lower as is the case with Nitrospira (1.9 ± 1.2 %); in this sample, the bacterial community composition was dominated by Hyphomicrobium (8.5 ± 1.0 %), Methylotenera (7.3 ± 6.5 %) and Methylophilus (6.3 ± 5.5 %). Different microplastic-attached bacterial assemblages within the several stages of WWTPs have previously been reported (Kelly et al., 2021). Tables S2 and S3 show the main water parameters of INF and EFL samples with relevant differences in NPOC, conductivity, ions (PO_4^{3-}, NH_4^+), and oxygen content; the observed differences in these water parameters, particularly nutrients may affect the microbial community in the plastisphere and could explain the observed differential bacterial composition of both water matrices (INF and EFL) as already shown by other authors (Hoellein et al., 2014; Arias-Andres et al., 2018; Oberbeckmann et al., 2018; Martínez-Campos et al., 2021). Regarding the microbial community in tMPs, tMPs-INF biofilm was dominated by Rhodanobacter (49.9 ± 1.5 %), Chitinophagaceae (11.3 ± 3.1 %), Mesorhizobium (8.3 ± 1.1 %), Parvibaculum (7.4 ± 0.3 %), whereas in tMPs-EFL, the most abundant were Gaiellales (5.3 ± 0.2 %), Rhizobacter (4.2 ± 0.5 %) and Rhodococcus (4.1 ± 0.5 %). These differences in relative abundance in the bacterial community revealed TCS-mediated shifts, as previously reported (Oh et al., 2019). The higher presence of Rhodanobacter in tMPs-INF in comparison to MPs-INF (< 1 %), or of the genus Rhodococcus in tMPs-EFL with respect to MPs-EFL (< 1 %), both with TCS-degrading members, suggests the selection of taxa with TCS-resistant and degrading abilities (Weatherly and Gosse, 2017; Oh et al., 2019; Leong et al., 2021; Yin et al., 2022). Although, at present, most studies on the TCS-degrading microbial community have used mainly high throughput methods such as metagenomics to directly study the microbial community structure and diversity, this is probably the first report of such potential TCS-biodegraders on biofouled plastics. Although it seems that TCS biodegradation is mainly through oxygenation to open the aromatic ring, and through dechlorination to carry out the biotransformation of toxic intermediates (Yin et al., 2022); the specific function of most TCS-degrading microorganisms has not been fully characterized and those bacteria forming part of the TCS-exposed plastisphere could be very interesting to analyze TCS-biodegradation in this new microbial habitat.

Fig. 3 shows the survival curves of *D. magna* exposed to PE-MPs in the absence of TCS (MPs-DW, MPs-Ec, MPs-INF, and MPs-EFL). The LT_{50} values are presented in Table S7 (SM). Significant differences with respect to the non-exposed control (LT_{50} = 17.0 ± 1.6) were found at the highest MPs concentrations: 200 mg/L and 400 mg/L for MPs-DW (LT_{50} < 11.0 ± 0.5 d), MPs-Ec (LT_{50} < 8.0 ± 2.7 d), and MPs-INF (LT_{50} < 9.0 ± 2.6 d), and from 100 mg/L upwards for MPs-EFL (LT_{50} < 6.0 ± 0.8 d) ($p < 0.05$). These results agree with the findings of Canniff and Hoang (2018) who tested the effect of fluorescent green pristine PE-MPs (63–75 µm) on *D. magna* adults reporting that concentrations as high as 100 mg/L did not sig-

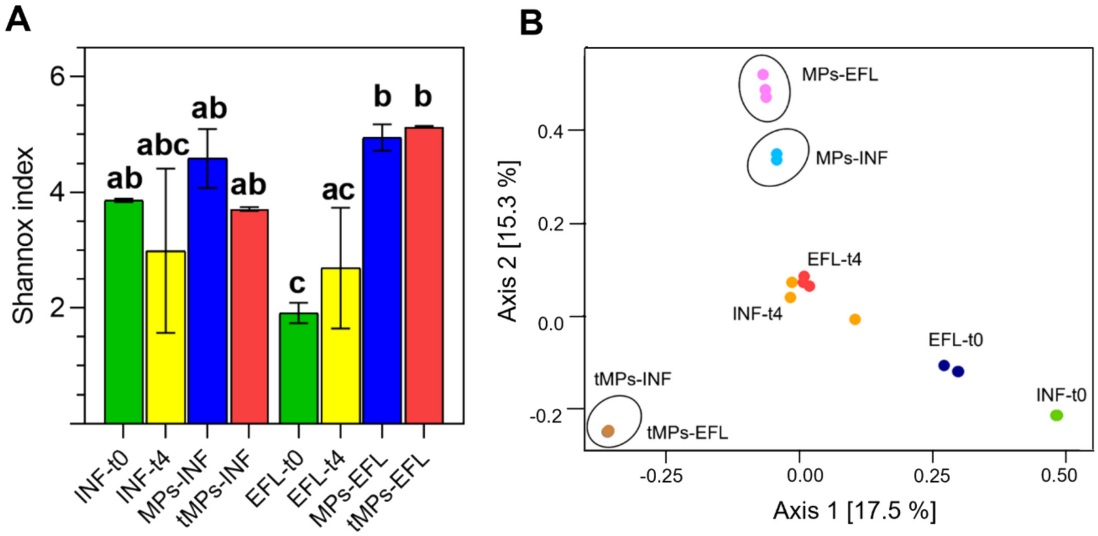

Figure 1: *α-diversity values using Shannox-Wienner index in all the substrates assayed: MPs-INF, MPs-EFL, tMPs-INF, and tMPs-EFL as well as INF and EFL water at the beginning (INF-t0 and EFL-t0) and at the end of biofouling experiments (INF-t4 and EFL-t4). Results are expressed as mean ± SD. Different letters indicated significant differences ($p < 0.05$) (A). B. β-diversity values using PCoA (principal coordinates analysis) plots for the bacterial composition in each sample based on Bray-Curtis dissimilarity. Percentages in axes represent % of variation explained by the axis. The ellipses encircle the samples from MPs and tMPs (B).*

nificantly affect survival (21 d) although the ingestion of MPs increased with concentration. Ingestion represents the main route of exposure of invertebrates to MPs (Aljaibachi and Callaghan, 2018; Canniff and Hoang, 2018). In this work, we found evidence of the accumulation of MPs in the digestive tract of daphnids in all treatments, except the non-exposed controls, as observed in the micrographs shown in Fig. S7 (SM). It has been pointed out that irregularly shaped plastics, which is the case in this study (Fig. S2B, SM), would increase residence time and induce higher damage (Frydkjær et al., 2017). Ma et al. (2016) also reported that PS-MPs (15 µm) at concentrations as high as 100 mg/L did not affect the immobilization of *D. magna* adults after 14 days of exposure. Kalčíková et al. (2020) studied the effect of pristine and naturally colonized PE-MPs (181 ± 119 µm) and found no effect on the survival of *D. magna* neonates after 48 h of exposure at a concentration of 100 mg/L. In Fig. S8, survival plots comparing biofouled and non-biofouled MPs at the same PE-MP concentrations are presented. For the lowest concentrations, 25 and 50 mg/L of MPs, there were no statistically significant differences in none of the scenarios tested. Nevertheless, at 100 mg/L, MPs-EFL (LT_{50} = 6.0 ± 0.8 d) showed significant differences with the rest of MPs ($p < 0.05$) (LT_{50} = 13.0 ± 1.1 d, MPs-DW; 13.0 ± 1.9 d, MPs-Ec; 15.0 ± 2.4 d, MPs-INF) showing that MPs-EFL were the most toxic PE-MPs for *D. magna* survival. Vroom et al. (2017) showed that aged microbeads (15–30 µm) were preferably ingested by zooplankton (copepods, *Calanus finmarchicus*, and *Acartia longiremis*) compared to pristine ones, probably due to the formation of a biofilm, the exudate of which may promote ingestion. The presence of biofilm could make plastic particles indistinguishable from natural food items (Zimmermann et al., 2020). This could explain the lower survival found in MPs-EFL with respect to MPs-DW, which were non-biofouled. The differences between MPs-INF and MPs-EFL could be explained based on MPs size distribution and the different nutritional quality of their respective biofilms (Siehoff et al., 2009; Horváthová and Bauchinger, 2019; Amariei et al., 2022). As shown in Table S8, there was a higher number of small PE-MP particles (20–40 µm) in MPs-EFL than in MPs-INF. This is the size range of particles that can be ingested by *D. magna* (Koelmans et al., 2020; Xu et al., 2020). It has been previously demonstrated that the toxicity of MPs decreases with increasing size. An et al. (2021) and Schwarzer et al. (2022) reported higher mortality, reduced body length, lower algal feeding rate, and offspring reduction in *D. magna* when the size of MPs decreased.

The total content of proteins, carbohydrates, and lipids in biofilms is shown in Table S9. The lower concentrations of these biomolecules (which are crucial for cellular processes) in MPs-EFL with respect to the concentrations of the same biomolecules in MPs-Ec and MPs-INF could also explain the observed differences in toxicity as biofilms growing in MPs-EFL are less nutritious. In this regard, bacterial taxonomy characterization revealed the lower presence of high-nutritional taxa such as the family Comamonaceae in MPs-EFL (1.07 ± 0.02 %) in comparison to MPs-INF (6.4 ± 0.1 %) as well as the growth of opportunistic bacteria like Pseudomonas which could be detrimental to *D. magna* survival (Le Coadic et

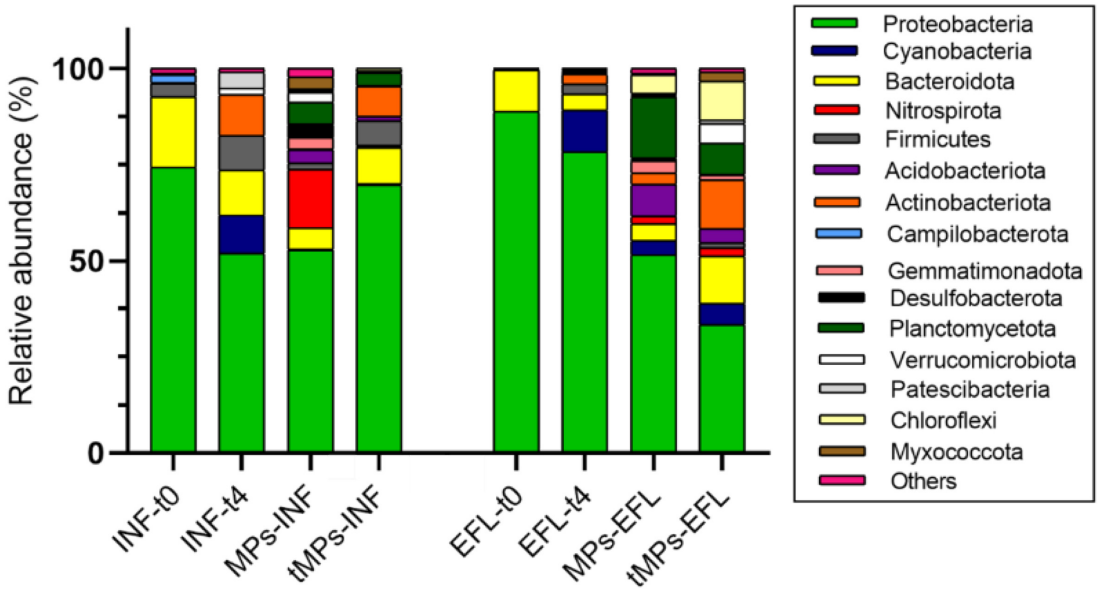

Figure 2: *Bacterial relative abundance at the phylum-level resolution in all the substrates assayed: MPs-INF and MPs-EFL, as well as their surrounding water at the beginning (INF-t0 and EFL-t0) and the end of the biofouling experiment (INF-t4 and EFL-t4).*

al., 2012; Callens et al., 2016; Mushegian et al., 2018) (Table S6, SM). Interestingly, although at a low abundance (0.10 ± 0.06 %), a symbiotic bacterial genus of *D. magna*, Flavobacterium, was reported in MPs-INF, but not in MPs-EFL (Qi et al., 2009; Freese and Martin-Creuzburg, 2013). The toxicity of the influent and effluent per se was also checked by exposing the organisms to wastewater (INF and EFL) for 21 d. Fig. S9 (SM) showed no difference in *D. magna* survival between both wastewaters. These data discard higher toxicity of the EFL itself due to possible different chemical compositions. To check the hypothesis that biofilms could act as carriers for toxic compounds, the amounts of certain microelements in the biofilm, including some toxic metals, were assessed. The concentration of all of them, as shown in Table S10 (SM), was higher in the INF, a result not consistent with a carrier or Trojan Horse effect of biofouled MPs to explain the higher toxicity of MPs-EFL. Furthermore, it was not possible to discard the possible bioaccumulation of toxic compounds from wastewater in biofilms that may increase their toxicity in effluent such as microelements (Table S10, SM) and possible organic chemical substances that could co-occur in wastewater.

The results of MPs previously exposed to TCS (tMPs) are presented in Fig. 4 and S10 (SM); and Table S7 (SM). The differences in survival were significant at lower concentrations as compared to non-exposed PE-MPs, from 50 mg/L for tMPs-DW (LT_{50}= 14.0 ± 1.4 d) ($p < 0.05$) and 100 mg/L for tMPs-Ec (13.0 ± 1.0 d) ($p < 0.05$). Remarkably, *D. magna* survival exposed to tMPs-EFL was significantly different from the control for all tested concentrations ($p < 0.05$). Increased mortality by tMPs-EFL was observed even for the lowest MPs concentration tested and from the first day of testing. On the contrary, tMPs-INF experiments resulted in significant differences with respect to the controls only and the highest concentrations tested (LT_{50} = 13.0 ± 1.3 d, 200 mg/L and 8.0 ± 1.0 d, 400 mg/L) ($p < 0.05$). The results showed that contrary to tMPs-EFL, tMPs-INF did not increase toxicity when pre-loaded with TCS.

The results of TCS sorption showed that MPs-DW sorbed 82.2 ± 0.4 µg TCS/g MPs after 4 h of exposure to the pollutant whereas the results for the other different media were: 57.2 ± 0.6 µg TCS/g MPs in MPs-Ec, 97.5 ± 1.6 µg TCS/g MPs in MPs-INF and of 88.0 ± 0.5 µg TCS/g MPs in MPs-EFL (Fig. 5A). Therefore, MPs-INF and MPs-EFL sorbed

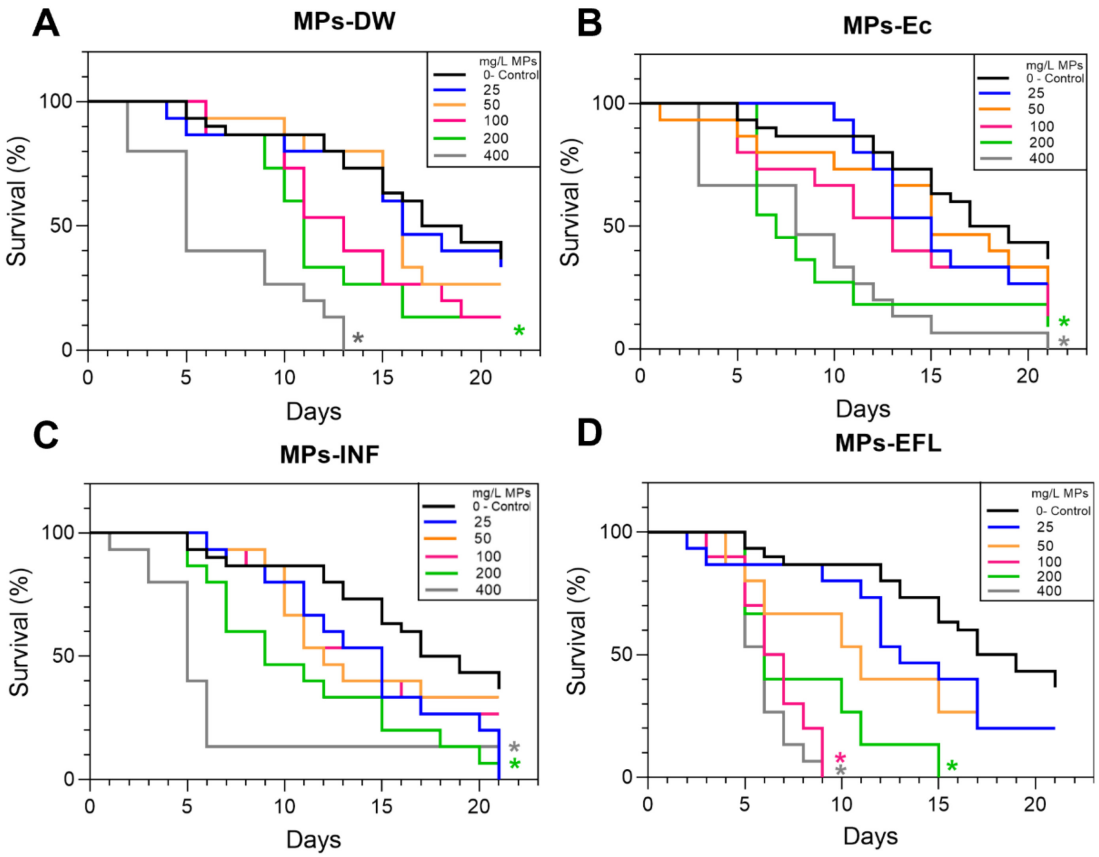

Figure 3: *Results of the Kaplan-Meier survival analysis for D. magna exposed for 21 days to concentrations of 0 (non-exposed control), 25, 50, 100, 200 and 400 mg/L of MPs-DW (A), MPs-Ec (B), MPs-INF (C), MPs-EFL (D). Asterisks (*) that appear to the right of each graph indicate whether there are significant differences ($p < 0.05$) with respect to the control.*

significantly higher amount of TCS ($p < 0.05$), being MPs-INF the MP with highest TCS sorption ($p < 0.05$). Other studies showed that biofilm formation considerably improved the sorption of pollutants, which included metals and organic pollutants (Richard et al., 2019; Wang et al., 2021). Wang et al. (2020), also reported that biofilm formation altered tetracycline and copper adsorption on PE MPs (60–150 μm), which was attributed to the larger specific surface area increases after biofilm growth. Likewise, Richard et al. (2019), showed that polylactic acid (PLA) and low-density polyethylene (LDPE) pellets (4–5 mm) recovered by estuarine biofilm, facilitated metal accumulation (Ba, Cs, Ge, Ga, Ni, and Rb). Specifically concerning TCS sorption, it has been shown that organic matter is the most influential factor in enhancing sorptivity in soils (Usyskin et al., 2015).

The interactions of organic pollutants and biofilms are largely determined by polar and electrostatic interactions. Therefore, the main physicochemical factors determining the amount of pollutant sorbed are those measuring their hydrophobicity–charge profile given by their pH-dependent octanol-water partition coefficient, D_{ow}, which in turn depends on pH and on the acid-base properties of the sorbate. Our results showed a sorption capacity for TCS in the following order: MPs-INF > MPs-EFL > MPs-DW > MPs-Ec, which agrees with the order of hydrophobicity determined by measuring the water contact angle of the MPs (Table S11, SM). These results are in agreement with the predominant role of hydrophobic interactions as the main driver for the retention of TCS, a hydrophobic compound (log K_{ow} = 4.76), non-dissociated at the working pH (pK_a = 8.1). The increase in hydrophobicity of plastic surfaces upon colonization has been observed before (Nauendorf et al., 2016). The lower sorption of TCS in MPs-Ec could be explained by the relatively high hydrophilicity of *E. coli* biofilms, which is consistent with a lower capacity to retain non-polar compounds, like TCS. The presence of polar groups in biofilms facilitates dipole interactions and hydrogen bonding in biofouled MPs in comparison with pristine surfaces (Ma et al., 2019; Liu et al., 2020). Accordingly, the higher hydrophobicity of MPs-INF and MPs-EFL (Table S11, SM), would explain their higher affinity to TCS.

The release of the biocide TCS in the liquid medium during the bioassays was also tested. The results are presented in Fig. 5B and showed a max-

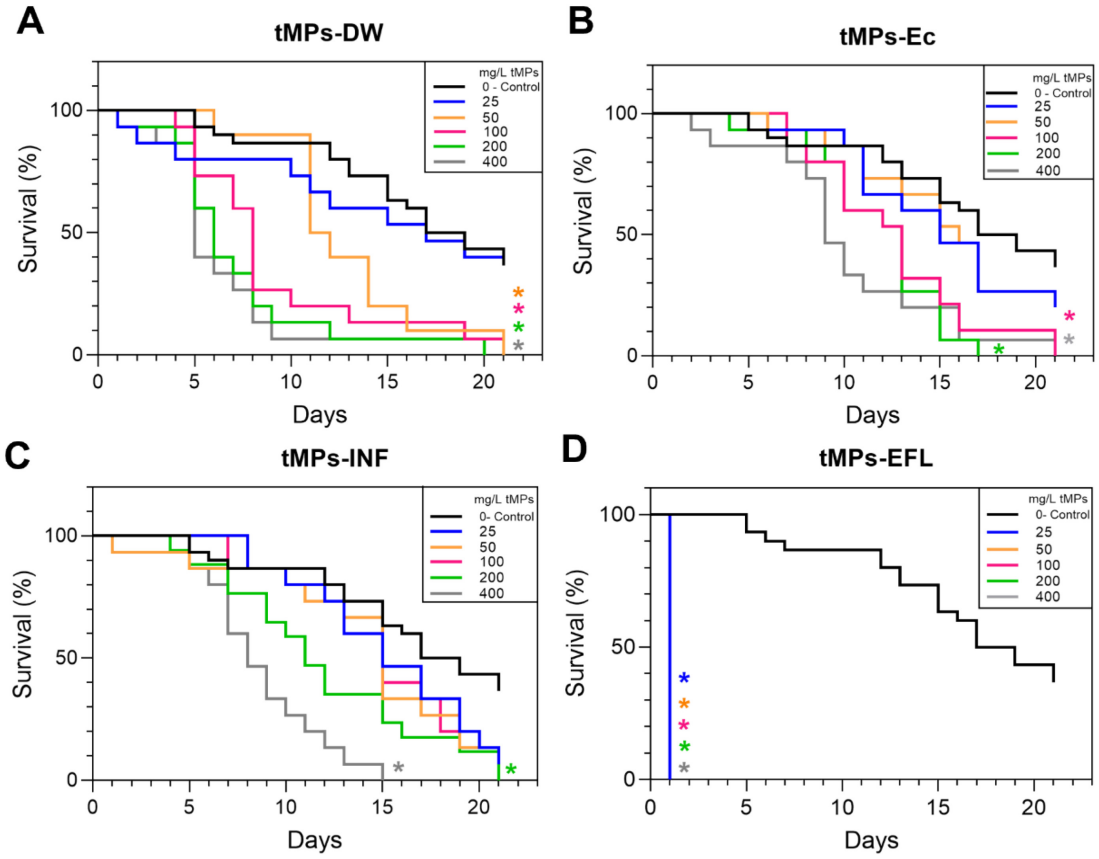

Figure 4: *Results of the Kaplan-Meier survival analysis for D. magna exposed for 21 days to concentrations of 0 (non-exposed control), 25, 50, 100, 200 and 400 mg/L of tMPs-DW (A), tMPs-Ec (B), tMPs-INF (C), tMPs-EFL (D). Asterisks (*) that appear to the right of each graph indicate whether there are significant differences ($p < 0.05$) with respect to the control.*

imum TCS concentration in the exposure medium of 28.4 ± 10.3 µg/L for tMPs-DW, which was only 12.8 ± 0.6 µg/L for tMPs-Ec. For MPs colonized in wastewater, tMPs-INF, and tMPs-EFL, TCS was only detected during the first few days of the assay (Fig. 5B). These results suggested that TCS could accumulate in or be degraded by the microbial biofilm formed on the surface of MPs. This could also explain that even though tMPs-INF retained a higher concentration of TCS, a corresponding higher toxicity was not observed.

Regarding the possible biodegradation of TCS taking place in the TCS-loaded PE-MP biofilms it is observed that genera such as Rhodanobacter, Rhodococcus, Nitrosomonas, Sphingomonas, and Sphingopyxis which have previously been pointed out as TCS degrading bacteria in wastewater were detected in a high abundance (>50 %) in tMPs-INF (Table S6, SM) (Hay et al., 2001; Roh et al., 2009; Lee et al., 2012). The capacity of biofilms formed on MPs to metabolize pollutants and, therefore, to reduce the associated toxicity, has been pointed out elsewhere (Rummel et al., 2017; Guan et al., 2020). Santos et al. (2019) studied the effect of TCS on river biofilms and reported its biotransformation into metabolites including methyl-TCS or 2.4-dichlorophenol. Peng et al. (2013) did not observe lethality in *D. magna* exposed for 21 days to TCS at concentrations in the water column up to 128 µg/L, and nor did Orvos et al. (2002), who reported that the NOEC based on survival at 21 d in the presence of TCS was 200 µg/L; higher concentrations of dissolved TCS than were observed in this study (Fig. 5B). Therefore, the toxicity observed in this work for tMPs in comparison to non-TCS-loaded MPs could be attributed to exposure via MPs ingestion, which contained sorbed TCS. Besides, the lower toxicity observed for tMPs-INF suggested biofilm degradation of TCS during the bioassays. In addition, a higher photolysis rate of TCS in waters with organic matter, such as wastewater, compared to ultrapure water has previously been indicated (Mezcua et al., 2004; Aranami and Readman, 2007). This could also contribute to explaining the absence of dissolved TCS in treatments with tMPs-INF and tMPs-EFL as compared to the other ones, indicating that most TCS remained in the biofilms (Fig. 5B), whose release is promoted by sorption equilibrium coefficient (K_{pw}) (Endo and Koelmans, 2019). In this regard, after 1 day of incubation, it was estimated that tMPs-EFL retained a higher concentration of TCS (34.7 ± 0.1 µg/g) in comparison to tMPs-INF (10 ± 2 µg/g) (Fig. 5B), what could explain the higher decrease in *D. magna* survival when exposed to tMPs-EFL.

The role of MPs as vectors of pollutants has been reported in previous studies. Frydkjær et al. (2017) found that irregular PE-MPs (10–75 µm) preincubated with phenanthrene were more toxic to *D. magna* than non-loaded MPs and that the EC_{50} could not be explained by the concentration of phenanthrene dissolved in the water column. Kalčíková et al. (2020) reported a toxic effect of silver to *D. magna* neonates enhanced on PE-MPs upon biofilm formation in contact with a natural water stream. Qi et al. (2021) demonstrated that the presence of biofilm in aged MPs enhanced the toxicity of lead to *D. magna*. Thus, according to our results, the higher observed toxicity of tMPs-DW, tMPs-Ec, and tMPs-EFL in comparison with non-TCS loaded PE-MPs was explained by the accumulation of TCS in the PE-MPs, particularly in tMPs-EFL. However, in the case of tMPs-INF, the lower toxicity could be due to the degradation of TCS by the microbial community and the better nutritional status of influent biofilms. Amariei et al. (2022) already found that *D. magna*

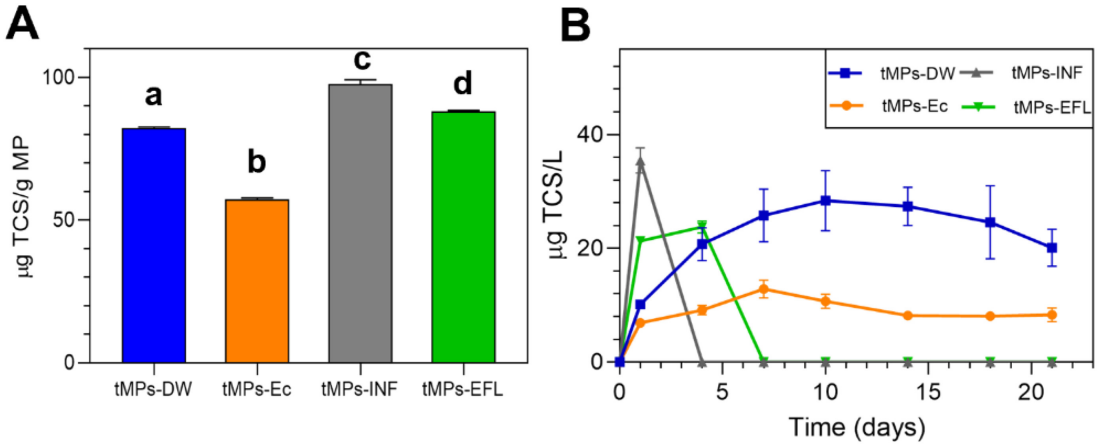

Figure 5: *Amount of sorbed TCS per unit dry mass of each tMPs (µg/g), tMPs-DW, tMPs-Ec, tMPs-INF, tMPs-EFL (A) and desorbed TCS concentration in the culture medium (µg/L) from TCS-loaded MPs, tMPs-DW, tMPs-Ec, tMPs-INF, and tMPs-EFL in a period of time of 21 days (B). In A, different letters indicate significant differences between treatments ($p < 0.05$). Results are shown as mean ± SD (n = 3).*

grew better when exposed to biofouled microplastics compared to pristine microplastics; however, this compensation due to biofilm-food supply was found only in MPs with the highest biofilm abundance (i.e., PE-MPS incubated in wastewater influent); in this regard, the higher toxicity observed with tMPs-EFL could be due to an increased TCS load as well as a lower nutrient supply within the attached biofilm.

It is known that MPs could be transferred along food chains from prey to predators (Huang et al., 2021). Moreover, due to predators requiring higher demands of energy, they could even be more affected by plastic pollution through ingestion. In the present study, *D. magna* ingested MPs, which were visualized in their digestive tracts, besides, MPs were also loaded with TCS. According to several authors who investigated the trophic transference of plastic particles, they were transferred from *D. magna* to predator fishes such as *Oryzias sinensis*, Zacco temminckii or *Carassius carassius* (Mattsson et al., 2017; Chae et al., 2018). Further research is required to know the possible bioaccumulation of TCS in these organisms. Besides, other studies have reported biomagnification along the trophic net in which the transfer of MPs and their associated chemicals has been demonstrated (Batel et al., 2016; Qu et al., 2020), it is thought that *D. magna* predators could be highly affected through the ingestion of their prey contaminated with MPs and TCS-loaded MPs. Given the importance of this primary consumer of phytoplankton as key prey for secondary consumers and its ecological role in freshwater ecosystems such as nutrient cycling, it is expected that its exposure to plastic pollution and associated chemicals may lead to a cascade of effects potentially harmful for higher- level organisms in the ecosystem (Miner et al., 2012).

4. Conclusions

The present work highlights that biofouling of microplastics influences their ability to adsorb and desorb co-occurring contaminants and thus, their potential role as vectors for the transport of them through aquatic environments. The microbial community analysis of the attached biofilms in biofouled microplastics is of paramount importance as it may modulate the nutritional status of the biofouled plastics as well as the amount of pollutant that may be sorbed and released from them and, subsequently the toxicity of the aquatic organisms that may ingest the biofouled plastics. Interestingly, the genomic analysis found potential triclosan-biodegrading taxa in the biofouled microplastics exposed to this pollutant. All these results imply that the tolerance of *D. magna* and possibly other aquatic organisms that might ingest microplastics is related to the degree of plastic biofouling in natural environments. In addition, such tolerance is also related to the sorption of co-occurring pollutants and their potential degradation by active organisms in the plastic-attached biofilm. Since plastic biofouling occurs over time in nature, future studies on realistic environmental plastic impact should include the characterization of the biofilms growing on plastic and how this may affect the sorption of co-occurring pollutants and subsequent toxicity towards biota.

Acknowledgements

The authors acknowledge the support provided by the Spanish Ministry of Science and Innovation, PID2020-113769RB-C21/22, PLEC2021-007693 (Funded by MCIN/AEI/10.13039/501100011033 and by the European Union "NextGenerationEU/PRTR") and TED2021-131609B-C32/33 grants, and the Thematic Network of Micro- and Nanoplastics in the Environment (RED2018-102345-T, EnviroPlaNet, www.enviroplanet.net). IV is the recipient of a predoctoral grant from the Spanish Ministry of Science (BES-2017-080711).

References

Aljaibachi, R., Callaghan, A., 2018. Impact of polystyrene microplastics on *Daphnia magna* mortality and reproduction in relation to food availability. PeerJ 6, e4601.

Amaral-Zettler, L.A., Zettler, E.R., Slikas, B., Boyd, G.D., Melvin, D.W., Morrall, C.E., Proskurowski, G., Mincer, T.J., 2015. The biogeography of the Plastisphere: implications for policy. Front. Ecol. Environ. 13, 541–546.

Amaral-Zettler, L.A., Zettler, E.R., Mincer, T.J., 2020. Ecology of the plastisphere. Nat. Rev. Microbiol. 18, 139–151.

Amariei, G., Rosal, R., Fernández-Piñas, F., Koelmans, A.A., 2022. Negative food dilution and positive biofilm carrier effects of microplastic ingestion by *D. magna* cause tipping points at the population level. Environ. Pollut. 294, 118622.

An, D., Na, J., Song, J., Jung, J., 2021. Size-dependent chronic toxicity of fragmented polyethylene microplastics to *Daphnia magna*. Chemosphere 271, 129591.

Andrady, A.L., 2017. The plastic in microplastics: a review. Mar. Pollut. Bull. 119, 12–22.

Aranami, K., Readman, J.W., 2007. Photolytic degradation of triclosan in freshwater and seawater. Chemosphere 66, 1052–1056.

Arias-Andres, M., Kettner, M.T., Miki, T., Grossart, H.P., 2018. Microplastics: new substrates for het-

erotrophic activity contribute to altering organic matter cycles in aquatic ecosystems. Sci. Total Environ. 635, 1152–1159.

Batel, A., Linti, F., Scherer, M., Erdinger, L., Braunbeck, T., 2016. Transfer of benzo [a] pyrene from microplastics to *Artemia nauplii* and further to zebrafish via a trophic food web experiment: CYP1A induction and visual tracking of persistent organic pollutants. Environ. Toxicol. Chem. 35, 1656–1666.

Borrelle Stephanie, B., Ringma, J., Law Kara, L., Monnahan Cole, C., Lebreton, L., McGivern, A., Murphy, E., Jambeck, J., Leonard George, H., Hilleary Michelle, A., Eriksen, M., Possingham Hugh, P., De Frond, H., Gerber Leah, R., Polidoro, B., Tahir, A., Bernard, M., Mallos, N., Barnes, M., Rochman Chelsea, M., 2020. Predicted growth in plastic waste exceeds efforts to mitigate plastic pollution. Science 369, 1515–1518.

Browne, M.A., Crump, P., Niven, S.J., Teuten, E., Tonkin, A., Galloway, T., Thompson, R., 2011. Accumulation of microplastic on shorelines woldwide: sources and sinks. Environ.Sci.Technol. 45, 9175–9179.

Browne, Mark A., Niven, Stewart J., Galloway, Tamara S., Rowland, Steve J., Thompson, Richard C., 2013. Microplastic moves pollutants and additives to worms, reducing functions linked to health and biodiversity. Curr. Biol. 23, 2388–2392.

Callens, M., Macke, E., Muylaert, K., Bossier, P., Lievens, B., Waud, M., Decaestecker, E., 2016. Food availability affects the strength of mutualistic host–microbiota interactions in *Daphnia magna*. ISME J. 10, 911–920.

Canniff, P.M., Hoang, T.C., 2018. Microplastic ingestion by *Daphnia magna* and its enhancement on algal growth. Sci. Total Environ. 633, 500–507.

Carson, H.S., 2013. The incidence of plastic ingestion by fishes: from the prey's perspective. Mar. Pollut. Bull. 74, 170–174.

Chae, Y., Kim, D., Kim, S.W., An, Y.J., 2018. Trophic transfer and individual impact of nano-sized polystyrene in a four-species freshwater food chain. Sci. Rep. 8, 1–11.

Chen, X., Nielsen, J.L., Furgal, K., Liu, Y., Lolas, I.B., Bester, K., 2011. Biodegradation of triclosan and formation of methyl-triclosan in activated sludge under aerobic conditions. Chemosphere 84, 452–456.

Cole, M., Lindeque, P., Halsband, C., Galloway, T.S., 2011. Microplastics as contaminants in the marine environment: a review. Mar. Pollut. Bull. 62, 2588–2597.

De Coen, W.M., Janssen, C.R., 1997. The use of biomarkers in *Daphnia magna* toxicity testing IV. Cellular energy allocation: a new methodology to assess the energy budget of toxicantstressed Daphnia populations. J. Aquat. Ecosyst. Stress. Recover. 6, 43–55.

de Ruijter, V.N., Redondo-Hasselerharm, P.E., Gouin, T., Koelmans, A.A., 2020. Quality criteria for microplastic effect studies in the context of risk assessment: a critical review. Environ.Sci.Technol. 54, 11692–11705.

de Sá, L.C., Oliveira, M., Ribeiro, F., Rocha, T.L., Futter, M.N., 2018. Studies of the effects of microplastics on aquatic organisms: what do we know and where should we focus our efforts in the future? Sci. Total Environ. 645, 1029–1039.

Eerkes-Medrano, D., Thompson, R.C., Aldridge, D.C., 2015. Microplastics in freshwater systems: a review of the emerging threats, identification of knowledge gaps and prioritisation of research needs. Water Res. 75, 63–82.

Endo, S., Koelmans, A.A., 2019. Sorption of hydrophobic organic compounds to plastics in the marine environment: equilibrium. In: Takada, H., Karapanagioti, H.K. (Eds.), Hazardous Chemicals Associated with Plastics in the Marine Environment. Springer International Publishing, Cham, pp. 185–204.

Free, C.M., Jensen, O.P., Mason, S.A., Eriksen, M., Williamson, N.J., Boldgiv, B., 2014. High-levels of microplastic pollution in a large, remote, mountain lake. Mar. Pollut. Bull. 85, 156–163.

Freese, H.M., Martin-Creuzburg, D., 2013. Food quality of mixed bacteria–algae diets for *Daphnia magna*. Hydrobiologia 715, 63–76.

Frydkjær, C.K., Iversen, N., Roslev, P., 2017. Ingestion and egestion of microplastics by the Cladoceran *Daphnia magna*: effects of regular and irregular shaped plastic and sorbed phenanthrene. Bull. Environ. Contam. Toxicol. 99, 655–661.

Geyer, R., 2020. Chapter 2 - production, use, and fate of synthetic polymers. In: Letcher, T.M. (Ed.), Plastic Waste and Recycling. Academic Press, pp. 13–32.

Geyer, R., Jambeck, J.R., Law, K.L., 2017. Production, use, and fate of all plastics ever made. Sci. Adv. 3, e1700782.

González-Pleiter, M., Pedrouzo-Rodríguez, A., Verdú, I., Leganés, F., Marco, E., Rosal, R., Fernández-Piñas, F., 2021. Microplastics as vectors of the antibiotics azithromycin and clarithromycin: effects towards freshwater microalgae. Chemosphere 268, 128824.

Guan, J., Qi, K., Wang, J., Wang, W., Wang, Z., Lu, N., Qu, J., 2020. Microplastics as an emerging

anthropogenic vector of trace metals in freshwater: significance of biofilms and comparison with natural substrates. Water Res. 184, 116205.

Hartmann, N.B., Rist, S., Bodin, J., Jensen, L.H., Schmidt, S.N., Mayer, P., Meibom, A., Baun, A., 2017. Microplastics as vectors for environmental contaminants: exploring sorption, desorption, and transfer to biota. Integr. Environ. Assess. Manag. 13, 488–493.

Hay, A.G., Dees, P.M., Sayler, G.S., 2001. Growth of a bacterial consortium on triclosan. FEMS Microbiol. Ecol. 36, 105–112.

Hoellein, T., Rojas, M., Pink, A., Gasior, J., Kelly, J., 2014. Anthropogenic litter in urban freshwater ecosystems: distribution and microbial interactions. PLOS ONE 9, e98485.

Horváthová, T., Bauchinger, U., 2019. Biofilm improves isopod growth independent of the dietary cellulose content. Physiol. Biochem. Zool. 92, 531–543.

Hosmer Jr., D.W., Lemeshow Jr., S., May Jr., S., 2008. Applied Survival Analysis: Regression Modelling of Time-to-Event Data, 2nd edition Wiley-Interscience, New York, USA, p. 416.

Huang, W., Song, B., Liang, J., Niu, Q., Zeng, G., Shen, M., Deng, J., Luo, Y., Wen, X., Zhang, Y., 2021. Microplastics and associated contaminants in the aquatic environment: a review on their ecotoxicological effects, trophic transfer, and potential impacts to human health. J. Hazard. Mater. 405, 124187.

Jacquin, J., Cheng, J., Odobel, C., Pandin, C., Conan, P., Pujo-Pay, M., Barbe, V., Meistertzheim, A.-L., Ghiglione, J.-F., 2019. Microbial ecotoxicology of marine plastic debris: a review on colonization and biodegradation by the "Plastisphere". Front. Microbiol. 10, 865.

Jemec Kokalj, A., Kuehnel, D., Puntar, B., Žgajnar Gotvajn, A., Kalčikova, G., 2019. An exploratory ecotoxicity study of primary microplastics versus aged in natural waters and wastewaters. Environ. Pollut. 254, 112980.

Kalčíková, G., Skalar, T., Marolt, G., Jemec Kokalj, A., 2020. An environmental concentration of aged microplastics with adsorbed silver significantly affects aquatic organisms. Water Res. 175, 115644.

Kay, P., Hiscoe, R., Moberley, I., Bajic, L., McKenna, N., 2018. Wastewater treatment plants as a source of microplastics in river catchments. Environ. Sci. Pollut. Res. 25, 20264–20267.

Kelly, J.J., London, M.G., McCormick, A.R., Rojas, M., Scott, J.W., Hoellein, T.J., 2021. Wastewater treatment alters microbial colonization of microplastics. PLOS ONE 16, e0244443.

Kelpsiene, E., Torstensson, O., Ekvall, M.T., Hansson, L.A., Cedervall, T., 2020. Long-term exposure to nanoplastics reduces life-time in *Daphnia magna*. Sci. Rep. 10, 5979.

Koelmans, A.A., Mohamed Nor, N.H., Hermsen, E., Kooi, M., Mintenig, S.M., De France, J., 2019. Microplastics in freshwaters and drinking water: critical review and assessment of data quality. Water Res. 155, 410–422.

Koelmans, A.A., Redondo-Hasselerharm, P.E., Mohamed Nor, N.H., Kooi, M., 2020. Solving the nonalignment of methods and approaches used in microplastic research to consistently characterize risk. Environ.Sci.Technol. 54, 12307–12315.

Lambert, S., Wagner, M., 2018. Microplastics are contaminants of emerging concern in freshwater environments: an overview. In: Wagner, M., Lambert, S. (Eds.), Freshwater Microplastics: Emerging Environmental Contaminants? Springer International Publishing, Cham, pp. 1–23.

Lambert, S., Scherer, C., Wagner, M., 2017. Ecotoxicity testing of microplastics: considering the heterogeneity of physicochemical properties. Integr. Environ. Assess. Manag. 13, 470–475.

Le Coadic, M., Simon, M., Marchetti, A., Ebert, D., Cosson, P., 2012. Daphnia magna, a host for evaluation of bacterial virulence. Appl. Environ. Microbiol. 78, 593–595.

Lee, D.G., Zhao, F., Rezenom, Y.H., Russell, D.H., Chu, K.H., 2012. Biodegradation of triclosan by a wastewater microorganism. Water Res. 46, 4226–4234.

Leong, Y.L., Krivak, D., Kiel, M., Laski, E., González-Sánchez, A., Dobslaw, D., 2021. Triclosan biodegradation performance of adapted mixed cultures in batch and continuous operating systems at high-concentration levels. Clean. Eng. Technol. 5, 100266.

Li, J., Liu, H., Paul Chen, J., 2018. Microplastics in freshwater systems: a review on occurrence, environmental effects, and methods for microplastics detection. Water Res. 137, 362–374.

Li, C., Busquets, R., Campos, L.C., 2020. Assessment of microplastics in freshwater systems: a review. Sci. Total Environ. 707, 135578.

Liu, P., Zhan, X., Wu, X., Li, J., Wang, H., Gao, S., 2020. Effect of weathering on environmental behavior of microplastics: properties, sorption and potential risks. Chemosphere 242, 125193.

Lobelle, D., Cunliffe, M., 2011. Early microbial biofilm formation on marine plastic debris. Mar. Pollut. Bull. 62, 197–200.

Ma, Y., Huang, A., Cao, S., Sun, F., Wang, L., Guo, H., Ji, R., 2016. Effects of nanoplastics and microplastics on toxicity, bioaccumulation, and en-

vironmental fate of phenanthrene in fresh water. Environ. Pollut. 219, 166–173.

Ma, J., Zhao, J., Zhu, Z., Li, L., Yu, F., 2019. Effect of microplastic size on the adsorption behavior and mechanism of triclosan on polyvinyl chloride. Environ. Pollut. 254, 113104.

Martínez-Campos, S., González-Pleiter, M., Fernández-Piñas, F., Rosal, R., Leganés, F., 2021. Early and differential bacterial colonization on microplastics deployed into the effluents of wastewater treatment plants. Sci. Total Environ. 757, 143832.

Mattsson, K., Johnson, E.V., Malmendal, A., Linse, S., Hansson, L.A., Cedervall, T., 2017. Brain damage and behavioural disorders in fish induced by plastic nanoparticles delivered through the food chain. Sci. Rep. 7, 1–7.

McCormick, A., Hoellein, T.J., Mason, S.A., Schluep, J., Kelly, J.J., 2014. Microplastic is an abundant and distinct microbial habitat in an urban river. Environ. Sci. Technol. 48, 11863–11871.

Mezcua, M., Gómez, M.J., Ferrer, I., Aguera, A., Hernando, M.D., Fernández-Alba, A.R., 2004. Evidence of 2, 7/2, 8-dibenzodichloro-p-dioxin as a photodegradation product of triclosan in water and wastewater samples. Anal. Chim. Acta 524, 241–247.

Miao, L., Wang, P., Hou, J., Yao, Y., Liu, Z., Liu, S., Li, T., 2019. Distinct community structure and microbial functions of biofilms colonizing microplastics. Sci. Total Environ. 650, 2395–2402.

Miner, B.E., De Meester, L., Pfrender, M.E., Lampert, W., Hairston Jr., N.G., 2012. Linking genes to communities and ecosystems: Daphnia as an ecogenomic model. Proc. R. Soc. B Biol. Sci. 279, 1873–1882.

Mosharaf, M.K., Tanvir, M.Z.H., Haque, M.M., Haque, M.A., Khan, M.A.A., Molla, A.H., Alam, M.Z., Islam, M.S., Talukder, M.R., 2018. Metal-adapted bacteria isolated from wastewaters produce biofilms by expressing proteinaceous curli fimbriae and cellulose nanofibers. Front. Microbiol. 9, 1334.

Murphy, F., Ewins, C., Carbonnier, F., Quinn, B., 2016. Wastewater treatment works (WwTW) as a source of microplastics in the aquatic environment. Environ.Sci.Technol. 50, 5800–5808.

Mushegian, A.A., Walser, J.-C., Sullam, K.E., Ebert, D., 2018. The microbiota of diapause: how host–microbe associations are formed after dormancy in an aquatic crustacean. J. Anim. Ecol. 87, 400–413.

Nauendorf, A., Krause, S., Bigalke, N.K., Gorb, E.V., Gorb, S.N., Haeckel, M., Wahl, M., Treude, T., 2016. Microbial colonization and degradation of polyethylene and biodegradable plastic bags in temperate fine-grained organic-rich marine sediments. Mar. Pollut. Bull. 103, 168–178.

Oberbeckmann, S., Kreikemeyer, B., Labrenz, M., 2018. Environmental factors support the formation of specific bacterial assemblages on microplastics. Front. Microbiol. 8, 2709.

OECD, 2012. Test No. 211: Daphnia magna Reproduction Test. OECD Guidelines for the Testing of Chemicals, Section 2. OECD Publishing, Paris.

OECD, 2022. Global Plastics Outlook: Economic Drivers, Environmental Impacts and Policy Options. OECD Publishing, Paris.

Ogonowski, M., Schür, C., Ogonowski, M., Schür, C., 2016. The effects of natural and anthropogenic microparticles on individual fitness in *Daphnia magna*. PLoS One 11, e0155063.

Oh, S., Choi, D., Cha, C.J., 2019. Ecological processes underpinning microbial community structure during exposure to subinhibitory level of triclosan. Sci. Rep. 9, 4598.

Orvos, D.R., Versteeg, D.J., Inauen, J., Capdevielle, M., Rothenstein, A., Cunningham, V., 2002. Aquatic toxicity of triclosan. Environ. Toxicol. Chem. 21, 1338–1349.

Peng, Y., Luo, Y., Nie, X.P., Liao, W., Yang, Y.F., Ying, G.-G., 2013. Toxic effects of triclosan on the detoxification system and breeding of Daphnia magna. Ecotoxicology 22, 1384–1394.

Phuong, N.N., Zalouk-Vergnoux, A., Poirier, L., Kamari, A., Châtel, A., Mouneyrac, C., Lagarde, F., 2016. Is there any consistency between the microplastics found in the field and those used in laboratory experiments? Environ. Pollut. 211, 111–123.

PlasticsEurope, 2021. Plastics—The Facts 2021: An Analysis of European Plastics Production, Demand and Waste Data. PlasticsEurope; Association of Plastics Manufacturers, Brussels, Belgium.

Qi, W., Nong, G., Preston, J.F., Ben-Ami, F., Ebert, D., 2009. Comparative metagenomics of Daphnia symbionts. BMC Genomics 10, 172.

Qi, K., Lu, N., Zhang, S., Wang, W., Wang, Z., Guan, J., 2021. Uptake of Pb (II) onto microplastic-associated biofilms in freshwater: adsorption and combined toxicity in comparison to natural solid substrates. J. Hazard. Mater. 411, 125115.

Qu, H., Ma, R., Barrett, H., Wang, B., Han, J., Wang, F., Chen, P., Peng, G., Yu, G., 2020. How microplastics affect chiral illicit drug methamphetamine in aquatic food chain? From green alga (*Chlorella pyrenoidosa*) to freshwater snail (*Cipangopaludian cathayensis*). Environ. Int. 136, 105480.

Richard, H., Carpenter, E.J., Komada, T., Palmer, P.T., Rochman, C.M., 2019. Biofilm facilitates metal accumulation onto microplastics in estuarine waters. Sci. Total Environ. 683, 600–608.

Rodrigues, A.C.M., Gravato, C., Quintaneiro, C., Golovko, O., Žlábek, V., Barata, C., Soares, A.M.V.M., Pestana, J.L.T., 2015. Life history and biochemical effects of chlorantraniliprole on *Chironomus riparius*. Sci. Total Environ. 508, 506–513.

Roh, H., Subramanya, N., Zhao, F., Yu, C.P., Sandt, J., Chu, K.-H., 2009. Biodegradation potential of wastewater micropollutants by ammonia-oxidizing bacteria. Chemosphere 77, 1084–1089.

Rummel, C.D., Jahnke, A., Gorokhova, E., Kühnel, D., Schmitt-Jansen, M., 2017. Impacts of biofilm formation on the fate and potential effects of microplastic in the aquatic environment. Environ.Sci.Technol.Lett. 4, 258–267.

Salta, M., Wharton, J.A., Blache, Y., Stokes, K.R., Briand, J.-F., 2013. Marine biofilms on artificial surfaces: structure and dynamics. Environ. Microbiol. 15, 2879–2893.

Santos, L.H.M.L.M., Freixa, A., Insa, S., Acuña, V., Sanchís, J., Farré, M., Sabater, S., Barceló, D., Rodríguez-Mozaz, S., 2019. Impact of fullerenes in the bioaccumulation and biotransformation of venlafaxine, diuron and triclosan in river biofilms. Environ. Res. 169, 377–386.

Savoca, M.S., Wohlfeil, M.E., Ebeler, S.E., Nevitt, G.A., 2016. Marine plastic debris emits a keystone infochemical for olfactory foraging seabirds. Sci.Adv. 2, e1600395.

Savoca, M.S., Tyson, C.W., McGill, M., Slager, C.J., 2017. Odours from marine plastic debris induce food search behaviours in a forage fish. Proc. R. Soc. B Biol. Sci. 284, 20171000.

Schwarzer, M., Brehm, J., Vollmer, M., Jasinski, J., Xu, C., Zainuddin, S., Fröhlich, T., Schott, M., Greiner, A., Scheibel, T., Laforsch, C., 2022. Shape, size, and polymer dependent effects of microplastics on Daphnia magna. J. Hazard. Mater. 426, 128136.

Siehoff, S., Hammers-Wirtz, M., Strauss, T., Ratte, H.T., 2009. Periphyton as alternative food source for the filter-feeding cladoceran Daphnia magna. Freshw. Biol. 54, 15–23.

Stevenson, K., McVey, A.F., Clark, I.B.N., Swain, P.S., Pilizota, T., 2016. General calibration of microbial growth in microplate readers. Sci. Rep. 6, 38828.

Tang, Y., Zhou, D., Su, L., Liu, Z., Zhang, X., Dumont, H.J., 2021. Vallisneria natans detritus supports Daphnia magna somatic growth and reproduction under addition of periphyton. Aquat. Ecol. 55, 579–588.

Trabelsi, L., M'sakni, N.H., Ben Ouada, H., Bacha, H., Roudesli, S., 2009. Partial characterization of extracellular polysaccharides produced by cyanobacterium Arthrospira platensis. Biotechnol. Bioprocess Eng. 14, 27–31.

Tu, C., Zhou, Q., Zhang, C., Liu, Y., Luo, Y., 2020. Biofilms of microplastics. In: He, D., Luo, Y. (Eds.), Microplastics in Terrestrial Environments: Emerging Contaminants and Major Challenges. Springer International Publishing, Cham, pp. 299–317.

Usyskin, A., Bukhanovsky, N., Borisover, M., 2015. Interactions of triclosan, gemfibrozil and galaxolide with biosolid-amended soils: effects of the level and nature of soil organic matter. Chemosphere 138, 272–280.

Verdú, I., González-Pleiter, M., Leganés, F., Rosal, R., Fernández-Piñas, F., 2021. Microplastics can act as vector of the biocide triclosan exerting damage to freshwater microalgae. Chemosphere 266, 129193.

Vroom, R.J.E., Koelmans, A.A., Besseling, E., Halsband, C., 2017. Aging of microplastics promotes their ingestion by marine zooplankton. Environ. Pollut. 231, 987–996.

Wang, Y., Wang, X., Li, Y., Li, J., Wang, F., Xia, S., Zhao, J., 2020. Biofilm alters tetracycline and copper adsorption behaviors onto polyethylene microplastics. Chem. Eng. J. 392, 123808.

Wang, J., Guo, X., Xue, J., 2021. Biofilm-developed microplastics as vectors of pollutants in aquatic environments. Environ.Sci.Technol. 55, 12780–12790.

Weatherly, L.M., Gosse, J.A., 2017. Triclosan exposure, transformation, and human health effects. J.Toxicol.Environ.Health Part B 20, 447–469.

Wu, C., Zhang, K., Huang, X., Liu, J., 2016. Sorption of pharmaceuticals and personal care products to polyethylene debris. Environ. Sci. Pollut. Res. 23, 8819–8826.

Wu, C., Tanaka, K., Tani, Y., Bi, X., Liu, J., Yu, Q., 2022. Effect of particle size on the colonization of biofilms and the potential of biofilm-covered microplastics as metal carriers. Sci. Total Environ. 821, 153265.

Xu, S., Ma, J., Ji, R., Pan, K., Miao, A.J., 2020. Microplastics in aquatic environments: occurrence, accumulation, and biological effects. Sci. Total Environ. 703, 134699.

Yang, L., Zhang, Y., Kang, S., Wang, Z., Wu, C., 2021. Microplastics in freshwater sediment: a review on methods, occurrence, and sources. Sci. Total Environ. 754, 141948.

Yin, Y., Wu, H., Jiang, Z., Jiang, J., Lu, Z., 2022. Degradation of triclosan in the water environment by

microorganisms: a review. Microorganisms 10, 1713.
Zettler, E.R., Mincer, T.J., Amaral-Zettler, L.A., 2013. Life in the "plastisphere": microbial communities on plastic marine debris. Environ.Sci.Technol. 47, 7137–7146.
Ziajahromi, S., Neale, P.A., Leusch, F.D.L., 2016. Wastewater treatment plant effluent as a source of microplastics: review of the fate, chemical interactions and potential risks to aquatic organisms. Water Sci. Technol. 74, 2253–2269.
Ziajahromi, S., Neale, P.A., Rintoul, L., Leusch, F.D.L., 2017. Wastewater treatment plants as a pathway for microplastics: development of a new approach to sample wastewater-based microplastics. Water Res. 112, 93–99.
Zimmermann, L., Göttlich, S., Oehlmann, J., Wagner, M., Völker, C., 2020. What are the drivers of microplastic toxicity? Comparing the toxicity of plastic chemicals and particles to *Daphnia magna*. Environ. Pollut. 267, 115392.

Supplementary Materials

Biofilm formation strongly influences the vector transport of triclosan-loaded polyethylene microplastics

Irene Verdú[1], Georgiana Amariei[2], Cristina Rueda-Varela[1], Miguel González-Pleiter[1], Francisco Leganés[1,3], Roberto Rosal[2], Francisca Fernández-Piñas[1,*]

[1]Department of Biology, Faculty of Science, Universidad Autónoma de Madrid, E-28049 Madrid, Spain
[2]Department of Chemical Engineering, Universidad de Alcalá, E-28871, Alcalá de Henares, Madrid, Spain
[3]Centro de Investigación en Biodiversidad y Cambio Global, Universidad Autónoma de Madrid. Darwin 2, 28049 Madrid, Spain

Contents:

*Corresponding author: francisca.pina@uam.es

Figure S1. Conceptual diagram of the experimental setup.

Figure S2. ATR-FTIR spectra (A), bright-field micrograph (B), and particle size distribution (C) of commercial PE-MPs.

Figure S3. Representative confocal micrographs of MPs-DW (A, B, C), MPs-Ec, (D, E, F), MPs-INF (G, H, I), and MPs-EFL (J, K, L), stained with FMTM 1-43 Green (A, D, F, J), SYPRO Ruby (B, E, H) and LIVE-DEAD (C, F, I, L) fluorochromes. Scale bars represent 50 µm.

Figure S4. Representative confocal micrographs of TCS-loaded MPs: tMPs-DW (A, B, C), tMPs-Ec, (D, E, F), tMPs-INF (G, H, I), and MPs-EFL (J, K, L), stained with FMTM 1-43 Green (A, D, F, J), SYPRO® Ruby (B, E, H) and LIVE-DEAD® (C, F, I, L) fluorochromes.

Figure S5. ATR-FTIR spectrum of commercial (original) MPs (MPs), and MPs-DW, MPs-Ec, MPs-INF, and MPs-EFL. Main regions with bands attributed to biofouling are highlighted, as well as the representative peaks of PE.

Figure S6. Rarefaction curves that compare the observed ASVs index in comparison with the number of reads for each sample (sequencing depth).

Figure S7. Microscopy images of the D. magna non-exposed to MPs (A, B, alive; C, D, dead specimens) and exposed to MPs (200 mg/L): MPs-DW (E-F), MPs-Ec (I, J), MPs-INF (M, N), MPs-EFL (Q, R). Likewise, D. magna exposed to TCS-loaded MPs (200 mg/L): tMPs-DW (G, H), tMPs-Ec (K, L), tMPs-INF (O, P), tMPs-EFL (S, T). Red arrows and circles indicate PE-MP particles.

Figure S8. Results of the Kaplan-Meier survival analysis for *D. magna* exposed for 21 days to concentrations of 0, 25 (A), 50 (B), 100 (C), 200 (D), and 400 (E) mg/L of MPs-DW, MPs-Ec, MPs-INF, MPs-EFL. The letters that appear to the right of each graph indicate if there are significant differences (p <0.05) or not between samples (different or same letter, respectively).

Figure S9. Results of the Kaplan-Meier survival analysis for *D. magna* exposed for 21 days to concentrations of 1:1 (A), 1:2 (B), and 1:4 (C) of wastewater from Influent (INF) and Effluent (EFL).

Figure S10. Results of the Kaplan-Meier survival analysis for *D. magna* exposed for 21 days to concentrations of 25 (A), 50 (B), 100 (C), 200 (D), and 400 (E) mg/L of tMPs-DW, tMPs-Ec, tMPs-INF, tMPs-EFL. The letters that appear to the right of each graph indicate if there are significant differences (p <0.05) or not between samples (different or same letter, respectively).

Supplementary Text 1. DNA Extraction and high-throughput sequencing. DNA was extracted from frozen samples of biofouled non-exposed, MPs-INF and MPs-EFL (50 mg) and exposed for 4 h to triclosan, tMPs-INF, and tMPs-EFL (50 mg) as well as water filters coming from the filtration of influent and effluent wastewater (1 L), at the beginning (INF-t0 and EFL-t0) and at the end of colonization time (4 weeks) (INF-t4 and EFL-t4). The procedure followed was essentially that described by Debeljak et al. (2017), adapted by Martínez-Campos et al. (2021), and with minor modifications. The DNA extraction was performed by triplicate and PE-MPs and water filters previously cut into small fragments with sterile scissors were added into 2 mL sterile Eppendorf tubes. Then, 400 µL of Tris-HCl 10 mM- EDTA 1 mM pH 8 and 20 µL of SDS 10 % (w/v) were added. After that, 250 µL of saturated phenol (pH 8) at 65 ºC, was also added and samples were vortexed for 1 min and incubated at 65 ºC, for 1 min. This last step was performed twice. After that, 250 µL chloroform was added, mixed for 30 s with vortex, and kept in ice for 30 s. These last steps were repeated three times. Subsequently, samples were centrifuged (13000 rpm) at 4 ºC for 15 min. The supernatants were recovered and transferred to new Eppendorf tubes, where 1 mL of hot saturated phenol (65 ºC) was added to clean the sample, vigorously shaking by hand. Samples were centrifuged again for 15 min, 13000 rpm at 4 ºC. The supernatants were recovered, and 1 mL chloroform was added to a clean Eppendorf tube. Carefully, the samples were mixed by hand and centrifugated for 15 min at 4 ºC. This step was performed twice. Following this, 400 µL of isopropanol were added to supernatants and kept overnight at -20 ºC to precipitate the DNA. Finally, samples were centrifuged for 30 min at 4 ºC and the supernatant was carefully discarded. The pellet was washed with 400 µL of ethanol 70 % and centrifuged (13000 rpm, 4 ºC, 10 min). The supernatant was removed, and the pellet was air-dried on a clean bench and resuspended with 10-20 µL sterile Milli-Q water. The DNA concentration and purity were measured using the spectrophotometer (NanoDrop ND-1000 Spectrophotometer). Samples were kept at -20 ºC until further analysis.

For metabarcoding analyses, PCR amplifications of the V3-V4 regions of the 16 rRNA of each sample were carried out by the Genomics Service of Parque Científico de Madrid (Madrid, Spain). For that, primers (100 nM), shown in Table S1 were used, and approximately 2-3 ng of DNA were also employed. The following conditions were followed for PCR amplifications: denaturalization at 98ºC for 30 s; followed by 23 cycles of denaturalization at 98 ºC for 30 s, annealing at 50 ºC for 20 s, and extension at 72 ºC for 20 s. The final elongation was at 72 ºC for 2 min. DNA was sequenced by a paired-end Illumina MiSeq 2x300 system according to the manufacturer's instructions obtaining at least 100000 reads per replicate.

Reads were initially processed using the DADA2 pipeline (1.16) in R software (4.1.3) for trimming, filtering, denoising and chimeras removing, and clustering into amplicon sequence variants (ASVs). For taxonomy assignments and abundances of each ASV, Qiime2 (Quantitative Insights Into Microbial Ecology 2) (2.2022) was used (McKinney, 2010, McDonald et al., 2012; Bolyen et al., 2019). The Silva reference database (Silva v138 SSURef_NR99) with 99 % homology was utilized. R software (v 4.1.3) was used for downstream analysis. Then, vegan (v 2.5-7) and phyloseq (v 1.38.0) packages were applied to calculate diversity measures; alpha-diversity based on Shannon-index; beta-diversity based on Bray-Curtis weighted distance. Analysis of variance (ANOVA), previously checking parametric assumptions, and post-hoc Tukey's HSD test was run to evaluate differences in Shannon-index between samples ($\alpha = 0.05$). In addition, permutational multivariate analysis of variance (PERMANOVA) using Bray-Curtis distance matrix with 999 permutations and Adonis function were used to test significant differences (*D. magna* < 0.05) between substrates (water and MPs), type of water (INF and EFL), the presence of TCS and time (t0 and t4) and their interactions. The package ggplot2 was run for visualization and graphics.

Bolyen, E., Rideout, J.R., Dillon, M.R., Bokulich, N.A., Abnet, C.C., Al-Ghalith, G.A., Alexander, H., Alm, E.J., Arumugam, M., Asnicar, F., et al., 2019. Reproducible, interactive, scalable and extensible microbiome data science using QIIME 2. Nature Biotechnology 37, 852-857.

Debeljak, P., Pinto, M., Proietti, M., Reisser, J., Ferrari, F.F., Abbas, B., van Loosdrecht, M.C.M., Slat, B., Herndl, G.J., 2017. Extracting DNA from ocean microplastics: a method comparison study. Analytical Methods 9, 1521-1526.

Martínez-Campos, S., González-Pleiter, M., Fernández-Piñas, F., Rosal, R., Leganés, F., 2021. Early and differential bacterial colonization on microplastics deployed into the effluents of wastewater treatment plants. Science of The Total Environment 757, 143832.

McDonald, D., Clemente, J.C., Kuczynski, J., Rideout, J.R., Stombaugh, J., Wendel, D., Wilke, A., Huse, S., Hufnagle, J., Meyer, F., Knight, R., Caporaso, J.G., 2012. The Biological Observation Matrix (BIOM) format or: how I learned to stop worrying and love the ome-ome. Gigascience 1, 7-7.

McKinney, W., 2010. Data structures for statistical computing in python. Proceedings of the 9th Python in Science Conference. Austin, TX, pp. 51-56.

Table S1. *Primers used in Illumina sequencing for 16S rRNA region.*

Target gene	Primer	Sequence (5′–3′)
16S rRNA	16SV3-V4-CS1	CCTACGGGNGGCWGCAG
	16SV3-V4-CS2	GACTACHVGGGTATCTAATCC

Table S2. *Main water parameters from distilled water (DW), E. coli culture medium (Ec), influent, and effluent at the beginning of the biofouling experiment (t = 0). Results are expressed as mean ± SD.*

			DW	Ec	Influent	Effluent
pH			7.5 ± 0.2	6.7 ± 0.1	8.2 ± 0.1	7.8 ± 0.3
Conductivity (µS/cm)			*	4.0 ± 0.2	383.7 ± 0.6	276 ± 1
O_2 (mg/L)			5.3 ± 0.1	4.9 ± 0.8	3.5 ± 0.2	5.0 ± 0.1
Dissolved NPOC (mg/L)			*	7223 ± 36	51.0 ± 0.7	8.7 ± 0.1
Total NPOC (mg/L)			*	8147 ± 43	67.1 ± 3.8	9.1 ± 0.5
OD_{600nm}			*	0.3 ± 0.1	0.21 ± 0.02	0.03 ± 0.01
OD_{260nm}			*	0.03 ± 0.01	3.40 ± 0.13	2.19 ± 0.43
Ions (mg/L)	Anions	F^-	n.d.	*	0.10 ± 0.05	0.10 ± 0.05
		ClO_2^-	n.d.	*	*	0.20 ± 0.05
		Cl^-	n.d.	3059 ± 22	54.0 ± 0.4	58.4 ± 0.4
		NO_2^-	n.d.	*	*	
		NO_3^-	n.d.	12.0 ± 0.5	*	50.8 ± 2.1
		PO_4^{3-}	n.d.	65.6 ± 2.1	8.7 ± 0.3	*
		SO_4^{2-}	n.d.	114.0 ± 0.6	39.1 ± 0.2	41.9 ± 0.2
	Cations	Na^+	n.d.	2226.7 ± 33.3	83.5 ± 1.2	61.8 ± 0.9
		NH_4^+	n.d.	40.7 ± 1.5	57.1 ± 2.0	*
		K^+	n.d.	162 ± 1	19.5 ± 0.2	15.4 ± 0.1
		Ca_2^+	n.d.	12.0 ± 0.2	48.3 ± 0.6	57.8 ± 0.8
		Mg_2^+	n.d.	36.4 ± 0.5	18.9 ± 2.3	17.7 ± 0.3

* Not different from zero; n.d.: Not determined

Table S3. *Main water parameters from distilled water (DW), E. coli culture (Ec), influent, and effluent at the end of the biofouling experiment (t = 4 weeks). Results are expressed as mean ± SD.*

			DW	Ec	Influent	Effluent
pH			8.4 ± 0.6	7.6 ± 0.01	8.3 ± 0.1	8.4 ± 0.1
Conductivity (µS/cm)			3.6 ± 0.9	1015.0 ± 32.9	834.7 ± 9.1	595 ± 13
O_2 (mg/L)			6.2 ± 0.1	0.10 ± 0.06	3.6 ± 1.0	6.2 ± 0.1
Dissolved NPOC (mg/L)			5.6 ± 0.1	6521 ± 61	269± 27	12.3 ± 0.2
Total NPOC (mg/L)			6.0 ± 0.1	10520 ± 5	323 ± 5	12.8 ± 0.1
OD_{600nm}			*	0.63 ± 0.05	0.04 ± 0.01	0.01 ± 0.00
OD_{260nm}			*	3.95 ± 0.09	3.56 ± 0.10	3.42 ± 0.04
Ions (mg/L)	Anions	F^-	0.25 ± 0.01	*	0.25 ± 0.01	0.17 ± 0.01
		ClO_2^-	0.42 ± 0.0	249 ± 3	0.50 ± 0.01	1.00 ± 0.01
		Cl^-	1.32 ± 0.01	3022 ± 22	57.4 ± 0.4	68.9 ± 5.0
		NO_2^-	0.14 ± 0.10	*	24.7 ± 10.7	*
		NO_3^-	2.0 ± 1.0	*	15.9 ± 0.7	63.0 ± 2.6
		PO_4^{3-}	n.d.	183.2 ± 6.0	8.9 ± 0.3	*
		SO_4^{2-}	2.3 ± 0.1	205.2 ± 1.0	42.3 ± 0.2	75.4 ± 0.4
	Cations	Na+	2.04 ± 0.03	2023 ± 30	85.4 ± 1.3	76.3 ± 1.1
		NH_4^+	n.d.	292 ± 11	32.0 ± 1.1	*
		K^+	n.d.	186 ± 1.4	16.7 ± 0.1	18.0 ± 0.1
		Ca^{2+}	4.2 ± 0.1	16 ± 0.2	30.2 ± 0.4	49.1 ± 0.7
		Mg^{2+}	0.61 ± 0.02	5.42 ± 0.08	13.5 ± 0.2	20.2 ± 0.3

* Not different from zero; n.d.: Not determined

Table S4. *Quality Assurance/Quality Control assessment, based on de Ruijter et al. (2020).*

Technical quality assessment		
Particle characterization		Score
1. Particle size	The particle size distribution of the commercial PE-MPs, and PE-MPs after biofouling and TCS exposure is indicated in Fig S2C and Table S8 respectively. A Beckman-coulter Z2 particle size analyzer was used for the measurements	2
2. Particle shape	Irregular shape. It was observed by an Olympus CX41 microscope with a digital colour camera Olympus DP20). A representative micrograph is presented in Fig. S2B	2
3. Polymer type	Polyethylene (PE). The material was checked by ATR-FTIR (ThermoScientific Nicolet iS10 apparatus with a Smart iTR-Diamond module). The spectrum is presented in Fig. S2A	2
4. Source of MPs	Commercial PE microplastics (MPs) were purchased from Sigma-Aldrich (CAS number 9002-88-4). Catalog number, 434272-100G. Lot number #MKCJ5757	2
5. Data reporting	MPs concentrations were reported in mg/L and particle number/L	2
Experimental Design		Score
6. Chemical purity	Prior to use, commercial PE-MPs were washed in methanol (100 %), under orbital shaking (1 h), and, later with distilled water three times and dried at 50 ºC overnight. So, chemical purity is assured, eliminating any artifactual chemical	2
7-8. Laboratory preparation & verification of contamination	To minimize plastic contamination during the manipulation and test exposure, all the instruments were previously washed with Milli-Q® water. Glass materials were preferably used to perform the test and keep the WW and PE-MPs solutions (Erlenmeyer flask, beakers, bottles...). Cotton lab coats were also used	2+2
9. Verification of exposure	To prepare and verify the exposure concentration of PE-MPs in biofouling assay (183.5 mg/L), PE-MPs powder from a commercial supplier was weighted in a precision balance and added to 2 L of different types of water (distilled water, *E. coli* culture, influent, and effluent wastewater), volume previously determined with a graduated cylinder. After biofouling time, PE-MPs were recovered by filtration and their dry weights were calculated to determine the exact mass of MPs recovered after aging time. A loss of 10 % was reported. So, using graduated cylinder and micropipettes, we got a stock solution of 10000 mg MPs/L and consequently, 25-400 mg MPs/L in bioassays	1
10. Homogeneity of exposure	Prior to assays, PE-MPs stock suspension was briefly ultrasonicated (Bioclock Scientific VibraCell 75042), whereas TCS stock solution was prepared in methanol (100 %) and shaken to assure a complete dissolution of the compound	2
11. Exposure assessment	By microscopy (Olympus CX41 microscope), the exposure of *D. magna* organisms to MPs and tMPs was observed. Representative pictures of the presence of MPs in their digestive tracts are shown in Fig. S7	2
12. Replication	A minimum of three replicates in each assay of this study (bioassays, MPs characterization, TCS sorption, metabarcoding) were run	2

Table S4 (Cont.). *Quality Assurance/Quality Control assessment, based on de Ruijter et al. (2020).*

Applicability in ecological risk assessment		
Applicable for Risk Assessment		Score
13. Endpoints	The survival of the organisms was chosen as the endpoint. This is an ecologically relevant endpoint to assess population-level risk (EPA 1996	2
14. Presence of natural (food) particles	*D. magna* organisms were fed with constant amounts (0.2 mg/L every two days) of the green algae *Chlamydomonas reinhardtii* in addition to extra nutrients coming from biofilm attached to PE-MPs	2
15-16. Reporting of effect thresholds and quality of the dose-response relationship	In bioassays, the adverse effects are reported as median lethal time (LT_{50}), according to the time-to-event data analysis of the experiment. Standard errors as well as 95 % confidence intervals were also indicated (Table S7	2+2
Ecological Relevance		Score
17. Concentration range tested	Organisms were exposed to 0, 25, 50, 100, 200 and 400 mg/L MPs and tMPs, which corresponds to 0, 2.13 x 10^6, 4.27 x 10^6, 8.54 x 10^6, 1.71 x 10^7, and 3.42 x 10^7 particles/L respectively. According to literature data it is estimated that their abundance in the freshwater environment varies depending on the site, having been detected in concentrations such as 0.0324-2.106 g/L in sediments; 0.0153-2.58 g/L in rivers, 0.27-1.74 g/L in lakes, and 0.288-0.468 g/L in estuaries being polyethylene (PE) on the most common polymer reported (Li et al., 2018; Li et al., 2020; Yang et al., 2021	2
18. Biofouling	MPs were biofouled in wastewater coming from an influent and effluent from a WWTP close to Madrid (Spain). Likewise, MPs were exposed to distilled water and *E. coli* cultures as negative and positive control of biofouling, respectively. The time exposure was 4 weeks at 25 ºC and 16/8 light/dark cycles in order to allow the formation of a substantial amount of biofilm	2
19. Diversity of PE-MPs tested	Polyethylene was the plastic polymer tested in these assays (Fig. S2A). The initial size distribution is shown in Fig S2C as well as the irregular morphology that the particles presented (Fig S2B	1
20. Exposure time	*D. magna* organisms were exposed to MPs for 21 days, the standardized recommended number of days for chronic tests by international toxicity guidelines (OECD 211)	2
Total Score		37

References for Table S4:

de Ruijter, V.N., Redondo-Hasselerharm, P.E., Gouin, T., Koelmans, A.A., 2020. Quality criteria for microplastic effect studies in the context of risk assessment: a critical review. Environmental Science & Technology 54, 11692-11705.

EPA, 1996. Ecological effects test guidelines OPPTS 850.1300 Daphnid chronic toxicity test. United States Environmental Protection Agency 712(C), 24.

Li, C., Busquets, R., Campos, L.C., 2020. Assessment of microplastics in freshwater systems: A review. Science of The Total Environment 707, 135578.

Li, J., Liu, H., Paul Chen, J., 2018. Microplastics in freshwater systems: A review on occurrence, environmental effects, and methods for microplastics detection. Water Research 137, 362-374.

OECD, 2012. Test No. 211: Daphnia magna Reproduction Test. OECD Guidelines for the testing of chemicals, Section 2, OECD Publishing, Paris.

Yang, L., Zhang, Y., Kang, S., Wang, Z., Wu, C., 2021. Microplastics in freshwater sediment: A review on methods, occurrence, and sources. Science of The Total Environment 754, 141948

Table S5. *PERMANOVA analysis using Bray-Curtis distance matrix for testing the factors substrate, WW, Time, and TCS in biofilm bacterial community. Bold numbers indicate significant differences (p <0.05).*

Factor	df	Sum of Squares	Mean of Squares	F	R^2	*p*-value
Substrate	1	1.3578	1.35779	7.2888	0.13551	0.001
WW	1	0.9295	0.92950	4.9897	0.09276	0.001
Time	1	1.1612	1.16122	6.2336	0.11589	0.001
TCS	1	1.6184	1.61841	8.6878	0.16152	0.001
Substrate x WW	1	0.8174	0.81738	5.4616	0.08157	0.001
WW x Time	1	0.7357	0.7357	4.9156	0.07342	0.001
WW x TCS	1	1.1552	1.15521	7.7190	0.11529	0.001
Substrate x WW x TCS	2	1.9726	0.98630	5.2946	0.19686	0.001
Substrate x WW x Time	1	0.7357	0.73567	4.9156	0.07342	0.001
Residuals	16	2.2449	0.14966		0.22404	
Total	22	10.0201			1.0000	

Table S6. *Most abundant (relative abundance > 1 %) bacterial taxa in MPs-INF, MPs-EFL, tMPs-INF and tMPs-EFL.*

MPs-INF	MPs-EFL	tMPs-INF	tMPs-EFL
Nitrospira (15.3 ± 1.1 %)	Hyphomicrobium (8.5 ± 1.0 %)	Rhodanobacter (49.9 ± 1.5 %)	Gaiellales (5.3 ± 0.2 %)
Dokdonella (7.9 ± 0.3 %)	Methylotenera (7.3 ± 6.5 %)	Chitinophagaceae (11.3 ± 3.1 %)	Rhizobacter (4.2 ± 0.5 %)
Arenimonas (6.3 ± 1.0 %)	Methylophilus (6.3 ± 5.5 %)	Mesorhizobium (8.3 ± 1.1 %)	Rhodococcus (4.1 ± 0.5 %)
Comamonadaceae * (3.4 ± 0.6 %)	Bryobacter (5.3 ± 3.8 %)	Parvibaculum (7.4 ± 0.3 %)	Caldilineaceae (3.9 ± 0.1 %)
Nitrosomonas (3.2 ± 1.3%)	SWB02 (4.4 ± 0.7 %)	Rhodococcus (4.2 ± 1.2 %)	Methylotenera (3.7 ± 0.6 %)
SWB02 (2.7 ± 0.6 %)	A0839 (3.7 ± 1.6 %)	Clostridium (3.5 ± 0.4 %)	Saprospiraceae (3.7 ± 0.2 %)
SM2D12 (2.7 ± 0.3 %)	Cellvibrionaceae (3.2 ± 2.8 %)	Actinobacteria PeM15 (2.8 ± 0.7 %)	Rhizobiaceae (3.7 ± 0.7 %)
Halomonas (2.6 ± 1.1%)	Gemmatimonadaceae (3.2 ± 1.6 %)	Hyphomicrobium (2.2 ± 0.1 %)	SJA-28 (3.4 ± 0.4 %)
Desulfomicrobium (2.6 ± 0.1 %)	SM1A02 (3.0 ± 1.8 %)	Rhizobiaceae (2.1 ± 0.1 %)	Arenimonas (3.2 ± 0.2 %)
Denitratisoma (2.2 ± 0.7 %)	Pirellulaceae (2.3 ± 1.4 %)	Xanthobacteraceae (1.8 ± 0.1 %)	SM1A02 (3.2 ± 0.1 %)
Nannocystis (1.8 ± 0.3 %)	Planctomycetales (2.2 ± 1.0 %)	Sphingomonas (1.8 ± 0.3 %)	Methylophilus (3.1 ± 0.3 %)
Gemmatimonadaceae_ (1.7 ± 0.4 %)	Saprospiraceae (2.0 ± 0.8 %)	Bradyrhizobium (1.7 ± 0.1 %)	Kouleothrix (3.1 ± 0.4 %)
Paludibaculum (1.5 ± 0.02 %)	Nitrospira (1.9 ± 1.2 %)	Coxiella (1.7 ± 0.5 %)	Gemmataceae (3.1 ± 0.5 %)
Gemmatimonas (1.3 ± 0.6 %)	Caldilineaceae (1.7 ± 1.9 %)	Romboutsia (1.7 ± 0.1 %)	Nitrospira (2.8 ± 0.2 %)
Pirellula (1.2 ± 0.1%)	Gemmataceae (1.6 ± 1.3 %)	Microbacteriaceae (1.4 ± 0.1 %)	Ferruginibacter (2.8 ± 0.7 %)
Micavibrionales_ (1.1 ± 0.2 %)	Alphaproteobacteria (1.4 ± 0.4 %)	Turicibacter (1.4 ± 0.1 %)	Lacunisphaera (2.5 ± 0.2 %)
Berkiella (1.1 ± 0.2 %)	Rhizobiaceae (1.3 ± 0.9 %)	Sphingomonadaceae (1.3 ± 0.1 %)	Prosthecobacter (2.3 ± 0.2 %)
	Gemmata (1.3 ± 0.9 %)	Paludibaculum (1.3 ± 0.3 %)	Caulobacter (2.2 ± 0.2 %)
	OM190 (1.3 ± 0.7 %)		Kapabacteriales (2.2 ± 0.2 %)
	Blastopirellula (1.2 ± 0.4 %)		1-20 (2.0 ± 0.1 %)
	Rhizobiales (1.1 ± 0.6 %)		Gemmatimonadaceae (1.5 ± 0.2 %)
	Reyranella (1.1 ± 0.3 %)		SBR1031 (1.4 ± 0.1 %)
	Pirellula (1.1 ± 0.3 %)		Bradyrhizobium (1.2 ± 0.2 %)
	Vicinamibacteraceae (1.0 ± 0.8 %)		Pirellulaceae (1.1 ± 0.2 %)
			Myxococcaceae (1.1 ± 0.2 %)
			Dechloromonas (1.7 ± 0.1 %)
			Microtrichales (1.0 ± 0.1 %)
			Bryobacter (1.0 ± 0.1 %)

Table S7. *Median lethal time (LT_{50}) of D. magna organisms exposed to different concentrations (0-400 mg/L) of MPs and TCS-loaded MPs (tMPs) in distilled water (DW), E. coli culture (Ec), and wastewater influent (INF,) and effluent (EFL). LT_{50} is given with standard errors (SE) and 95 % level confidence intervals (CI).*

		MPs				TCS-loaded MPs (tMPs)			
	mg MPs/L	LT_{50}	SE	CI (95 %)		LT_{50}	SE	CI (95 %)	
				Min	Max			Min	Max
Control	0	17.0	1.6	14.0	20.2	-	-	-	-
DW	25	16.0	1.9	12.2	19.8	17.0	1.5	13.9	18.3
	50	16.0	0.5	15.1	16.9	14.0	1.4	11.2	16.8
	100	13.0	1.1	10.8	15.2	8.0	0.3	7.3	8.7
	200	11.0	0.5	10.1	11.9	6.0	0.6	4.8	7.2
	400	5.0	0.9	3.1	6.9	5.0	0.5	3.9	6.1
Ec	25	15.0	1.1	12.8	17.2	15.0	1.5	12.0	18.0
	50	15.0	2.4	10.3	19.7	16.0	1.3	13.5	18.5
	100	13.0	1.9	9.3	16.7	13.0	1.5	10.1	15.9
	200	7.0	1.9	3.3	10.7	13.0	1.0	11.0	15.0
	400	8.0	2.7	2.7	13.3	9.0	0.6	7.7	10.3
INF	25	15.0	1.4	12.3	17.7	15.0	1.9	11.2	18.8
	50	12.0	0.6	9.2	14.8	15.0	0.7	13.6	16.4
	100	15.0	2.4	10.4	19.6	15.0	0.9	13.1	16.9
	200	9.0	2.6	4.0	14.0	13.0	1.2	10.7	15.3
	400	5.0	0.6	3.8	6.2	8.0	1.0	6.1	9.9
EFL	25	13.0	1.5	10.0	16.0	-	-	-	-
	50	11.0	2.4	6.4	15.6	-	-	-	-
	100	6.0	0.8	4.5	7.5	-	-	-	-
	200	6.0	0.5	5.1	6.9	-	-	-	-
	400	6.0	0.9	4.2	7.8	-	-	-	-

Table S8. *Size distribution of MPs non-exposed to TCS (MPs-DW, MPs-Ec, MPs-INF, and MPs-EFL); and TCS-loaded MPs (tMPs-DW, tMPs-Ec, tMPs-INF, and tMPs-EFL). A concentration of 50 mg/L of MPs was used. Mean standard deviation, 10 %.*

particles/mL	Treatment							
Size (µm)	MPs-DW	tMPs-DW	MPs-Ec	tMPs-Ec	MPs-INF	tMPs-INF	MPs-EFL	tMPs-EFL
10-20	3194	3337	2652	2456	1130	1130	1183	1189
20-30	914	946	765	823	256	256	632	404
30-40	674	619	632	608	421	322	549	592
40-50	188	318	216	258	289	182	216	224
50-60	105	98	89	90	48	70	64	72
60-70	12	6	0	4	16	21	16	8
70-80	0	0	0	0	2	0	0	0
80-90	0	0	0	0	0	0	0	0
90-100	0	0	0	0	0	0	0	0
10-100 µm	5087	5324	4354	4239	2162	1981	2660	2489

Table S9. *Total amount of proteins, carbohydrates, and lipids (mg) per g of MPs-DW, MPs-Ec, MPs-INF, MPs-EFL, and the TCS-loaded MPs: tMPs-DW, tMPs-Ec, tMPs-INF and tMPs-EFL. Results are expressed as mean ± SD.*

					TCS-loaded			
	MPs-DW	MPs-Ec	MPs-INF	MPs-EFL	tMPs-DW	tMPs-Ec	tMPs-INF	tMPs-EFL
Proteins (mg/g)	0	282.6 ± 4.5	61.2 ± 9.4	27.6 ± 4.8	0	229.1 ± 33.9	43.6 ± 7.1	8.4 ± 2.1
Carbohydrates (mg/g)	0	185.6 ± 1.9	139.8 ± 0.9	45.3 ± 0.4	0	191.3 ± 1.9	145.0 ± 0.9	43.1 ± 1.0
Lipids (mg/g)	0	25.6 ± 1.4	8.4 ± 1.3	4.4 ± 0.7	0	21.7 ± 1.2	8.9 ± 0.4	4.0 ± 0.1

Table S10. *Concentration of microelements (mg) per gram of MPs-INF and MPs-EFL as determined by TXRF. Results are expressed as mean ± SD.*

Element (mg/g)	Treatment	
	MPs-INF	MPs-EFL
P	2.631 ± 0.054	0.133 ± 0.026
Ti	1.076 ± 0.007	0.046 ± 0.002
Fe	1.164 ± 0.005	0.294 ± 0.002
Mn	0.031 ± 0.001	0.035 ± 0.001
Ni	0.007 ± 0.001	0.003 ± 0.001
Cu	0.051 ± 0.001	0.003 ± 0.001
Zn	0.182 ± 0.001	0.027 ± 0.001
Pb	0.023 ± 0.001	0.001 ± 0.001

Table S11. *Contact angle (CA, °) of MPs-DW, MPs-Ec, MPs-INF, MPs-EFL, and TCS-loaded MPs: tMPs-DW, tMPs-Ec, tMPs-INF, and tMPs-EFL as a measure of hydrophobicity. Results are expressed as mean ± SD.*

				TCS-loaded			
MPs-DW	MPs-Ec	MPs-INF	MPs-EFL	tMPs-DW	tMPs-Ec	tMPs-INF	tMPs-EFL
111.5±0.3	72.4±1.7	127±1.4	119.5 ± 0.7	111±1.4	73.2±0.56	123.6±0.5	122.9 ± 0.2

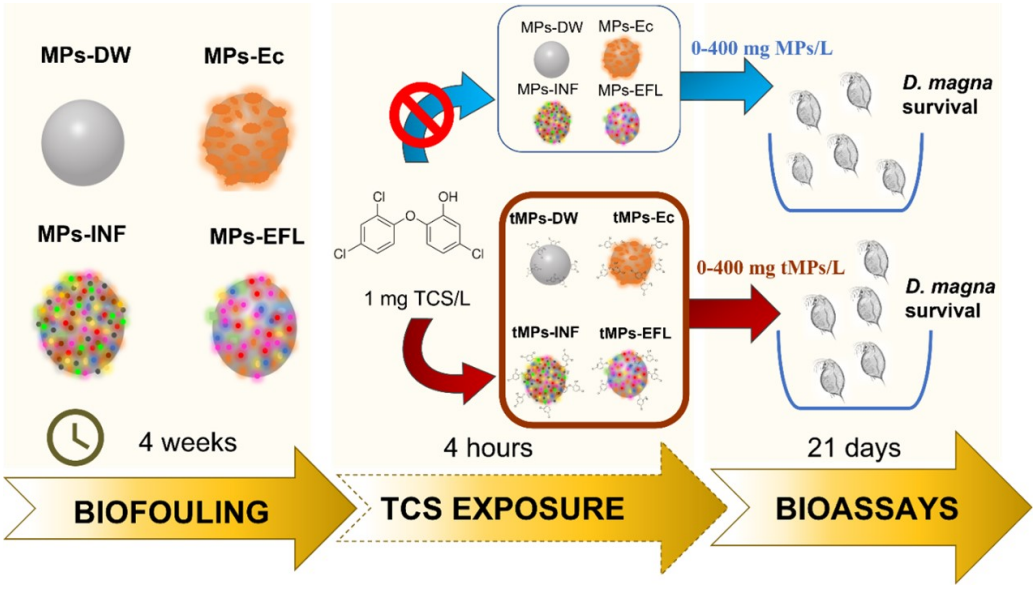

Figure S1: *Conceptual diagram of the experimental setup.*

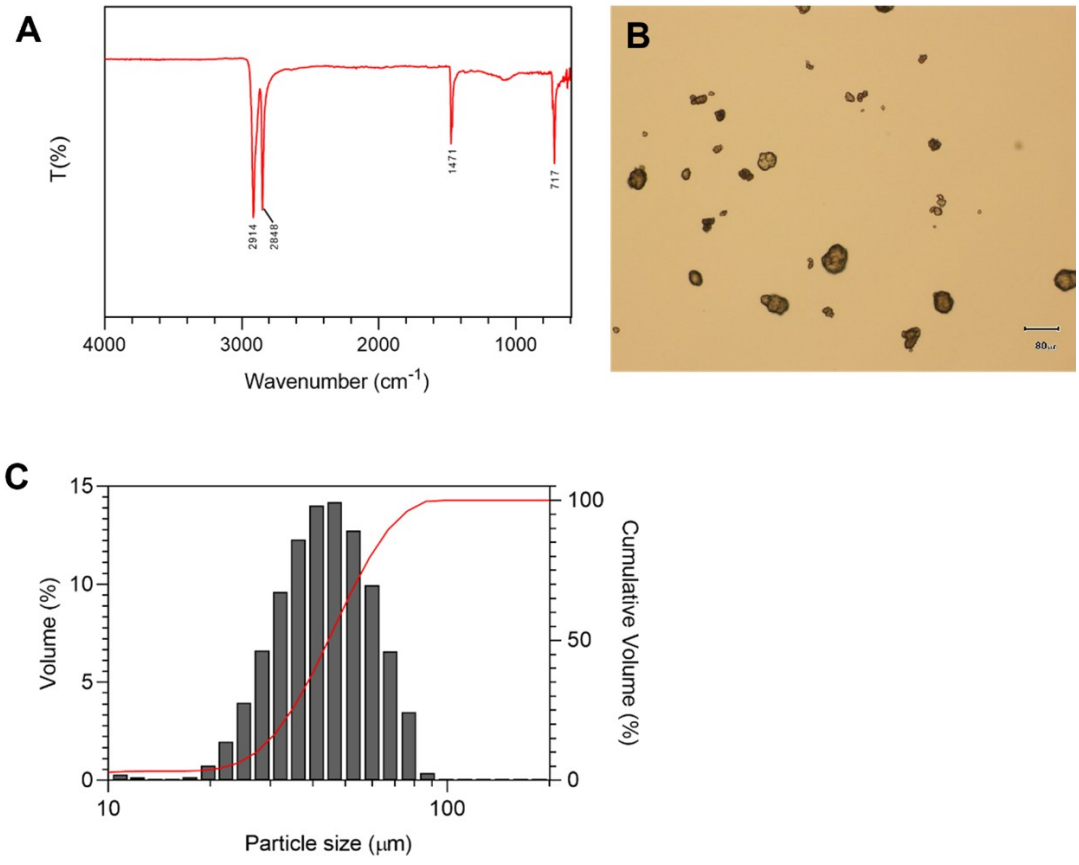

Figure S2: *ATR-FTIR spectra (A), bright-field micrograph (B), and particle size distribution (C) of commercial PE-MPs.*

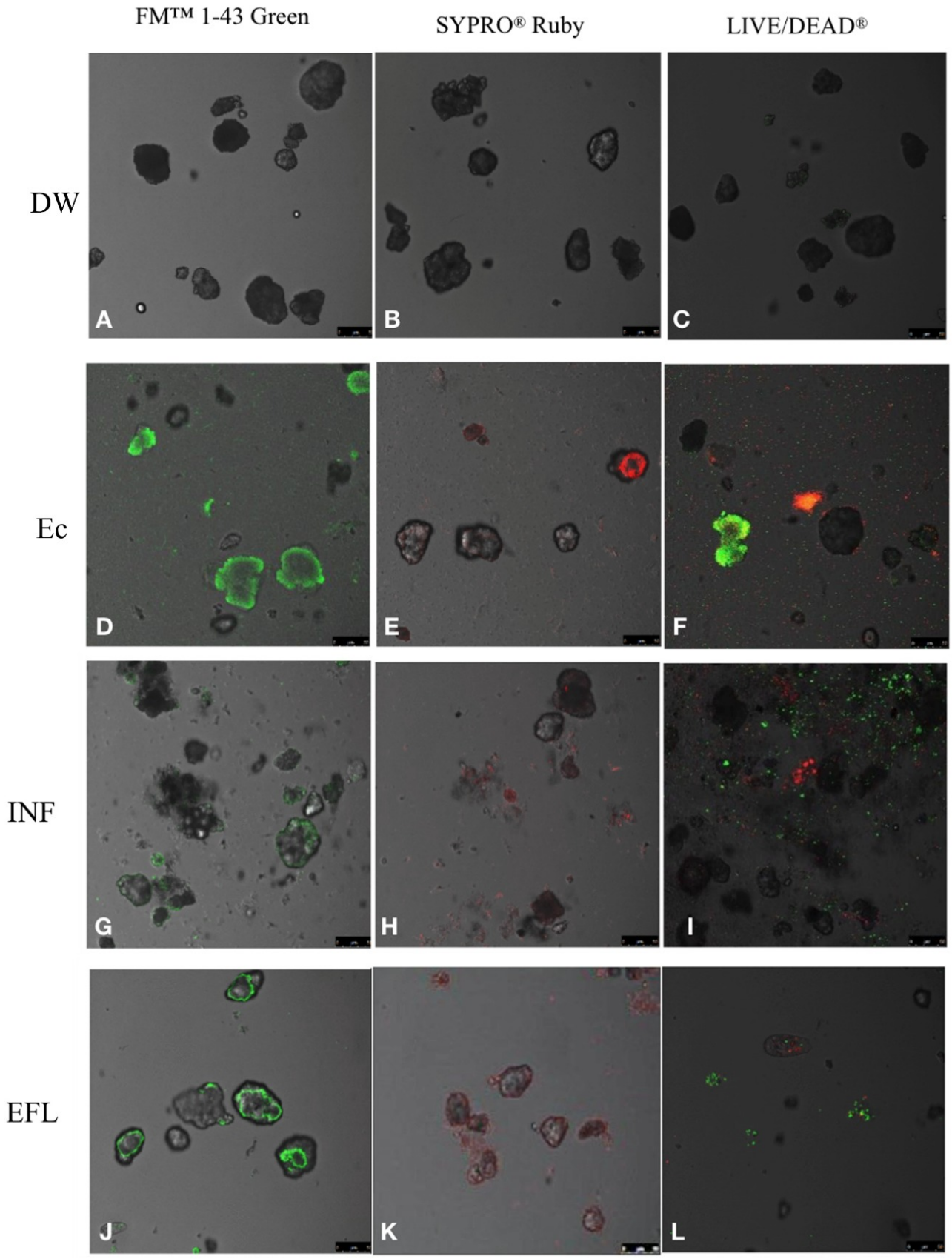

Figure S3: *Representative confocal micrographs of MPs-DW (A, B, C), MPs-Ec, (D, E, F), MPs-INF (G, H, I) and MPs-EFL (J, K, L), stained with FMTM 1-43 Green (A, D, F, J), SYPRO Ruby (B, E, H) and LIVE-DEAD (C, F, I, L) fluorochromes. Scale bars represent 50 µm.*

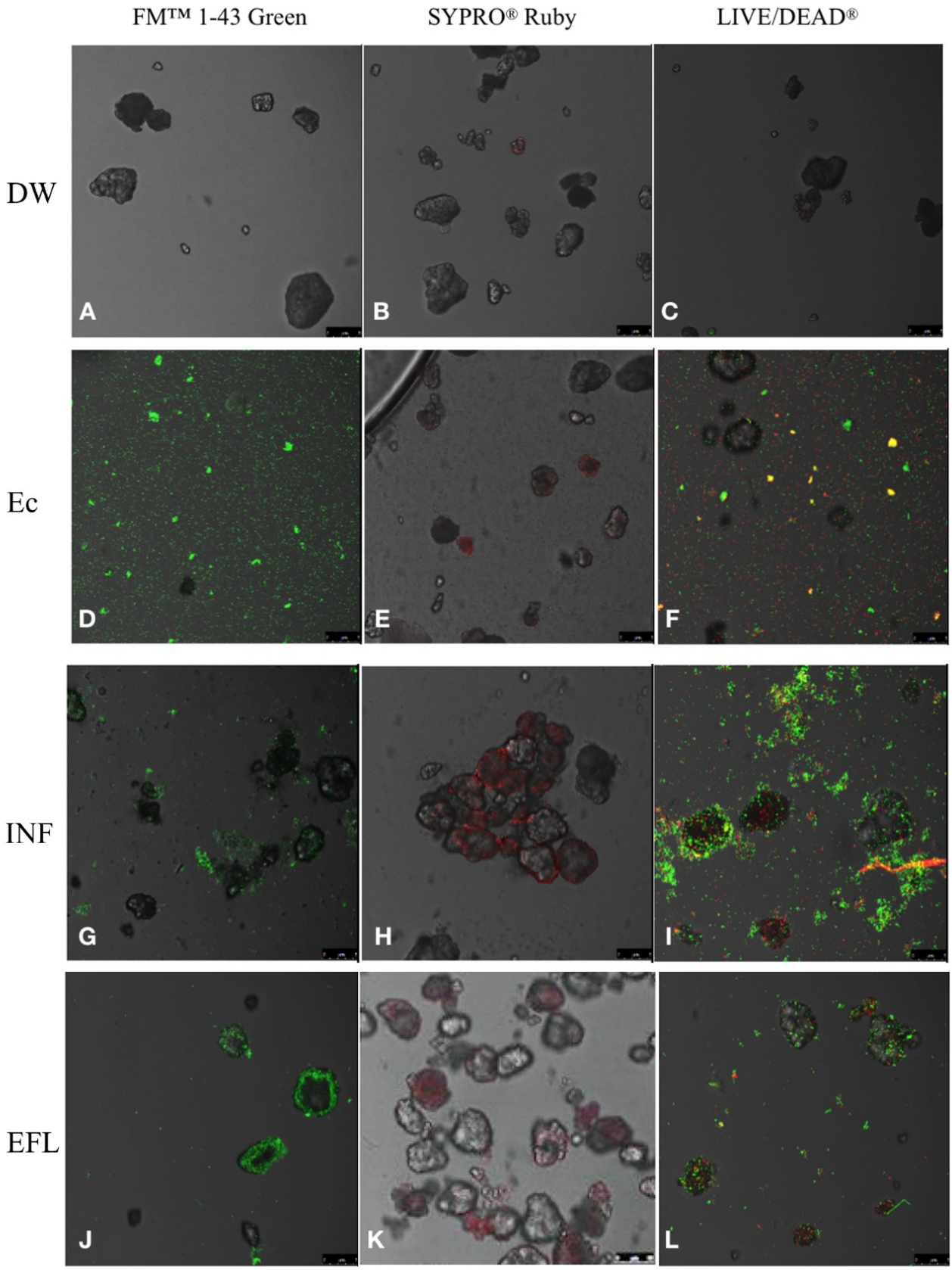

Figure S4: *Representative confocal micrographs of TCS-loaded MPs: tMPs-DW (A, B, C), tMPs-Ec, (D, E, F), tMPs-INF (G, H, I) and MPs-EFL (J, K, L), stained with FMTM 1-43 Green (A, D, F, J), SYPRO Ruby (B, E, H) and LIVE-DEAD (C, F, I, L) fluorochromes.*

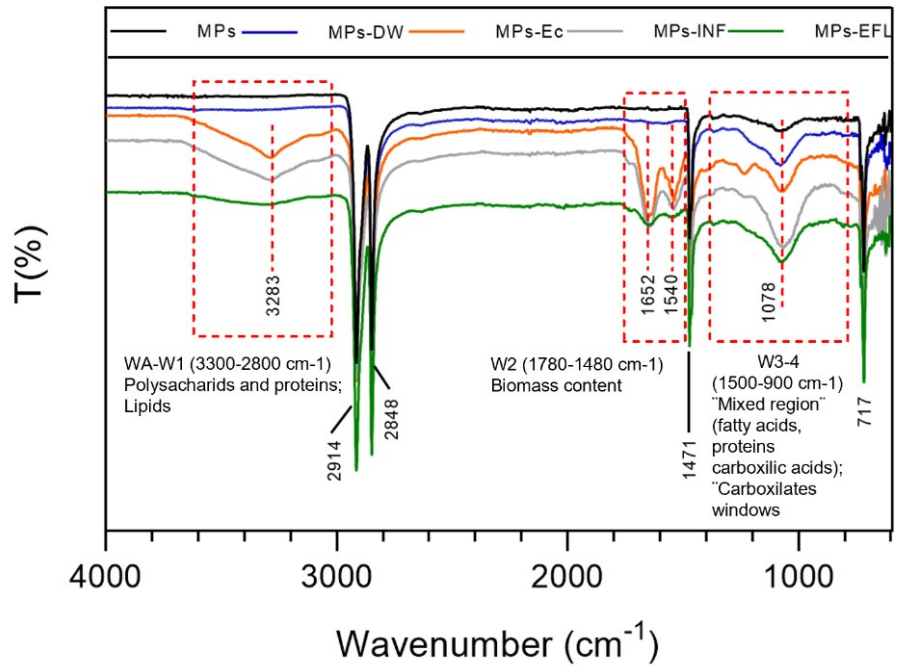

Figure S5: *ATR-FTIR spectrum of commercial (original) MPs (MPs), and MPs-DW, MPs-Ec, MPs-INF, and MPs-EFL. Main regions with bands attributed to biofouling are highlighted, as well as the representative peaks of PE.*

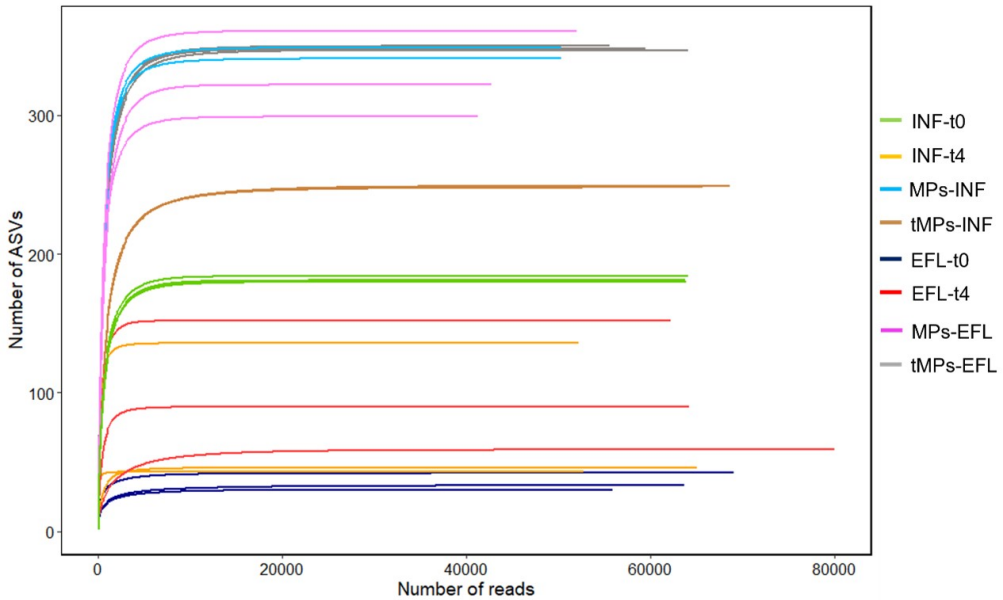

Figure S6: *Rarefaction curves that compare the observed ASVs index in comparison with the number of reads for each sample (sequencing depth).*

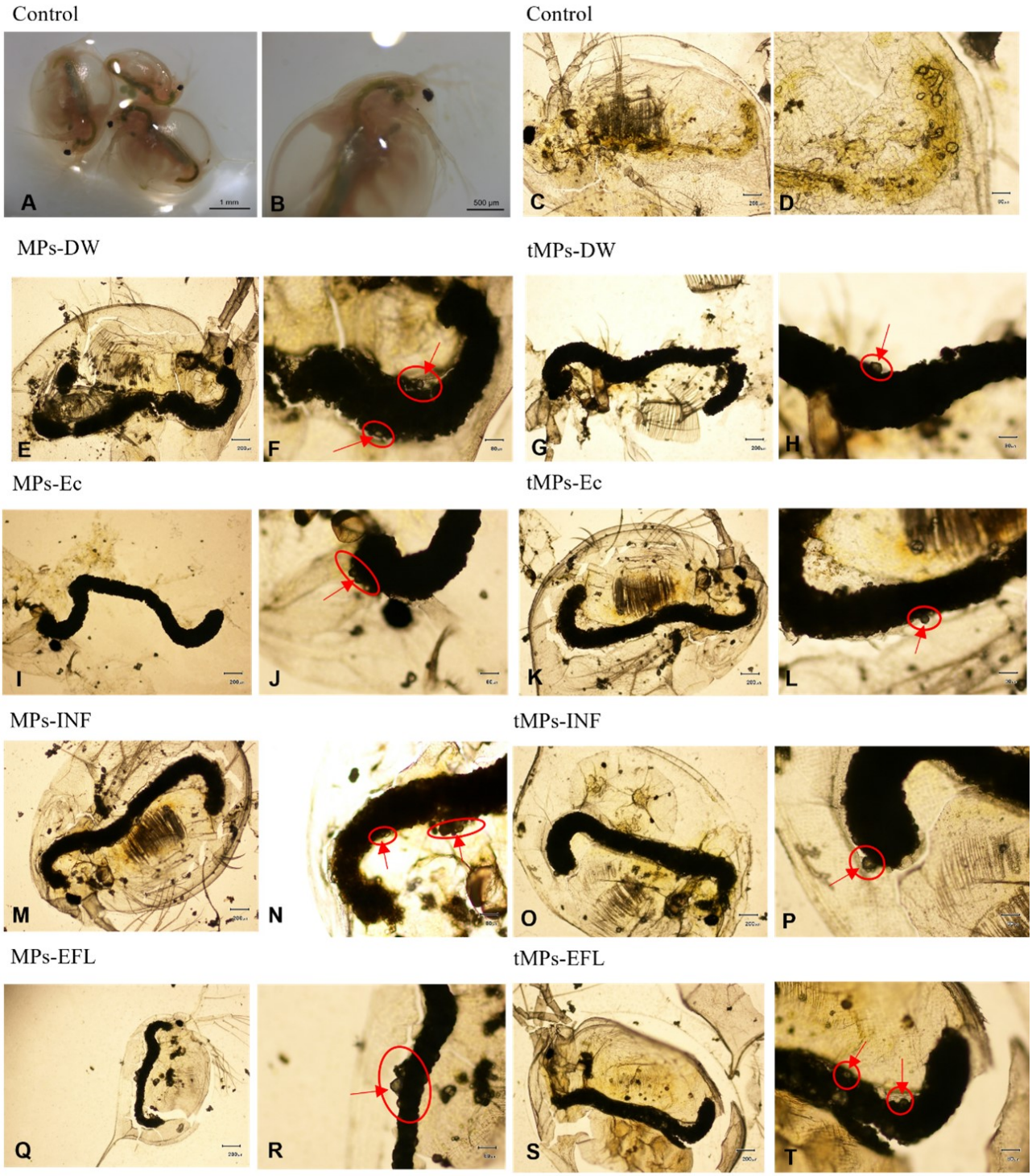

Figure S7: *Microscopy images of the D. magna non-exposed to MPs (A, B, alive; C, D, dead specimens) and exposed to MPs (200 mg/L): MPs-DW (E-F), MPs-Ec (I, J), MPs-INF (M, N), MPs-EFL (Q, R). Likewise, D. magna exposed to TCS-loaded MPs (200 mg/L): tMPs-DW (G, H), tMPs-Ec (K, L), tMPs-INF (O, P), tMPs-EFL (S, T). Red arrows and circles indicate MP particles.*

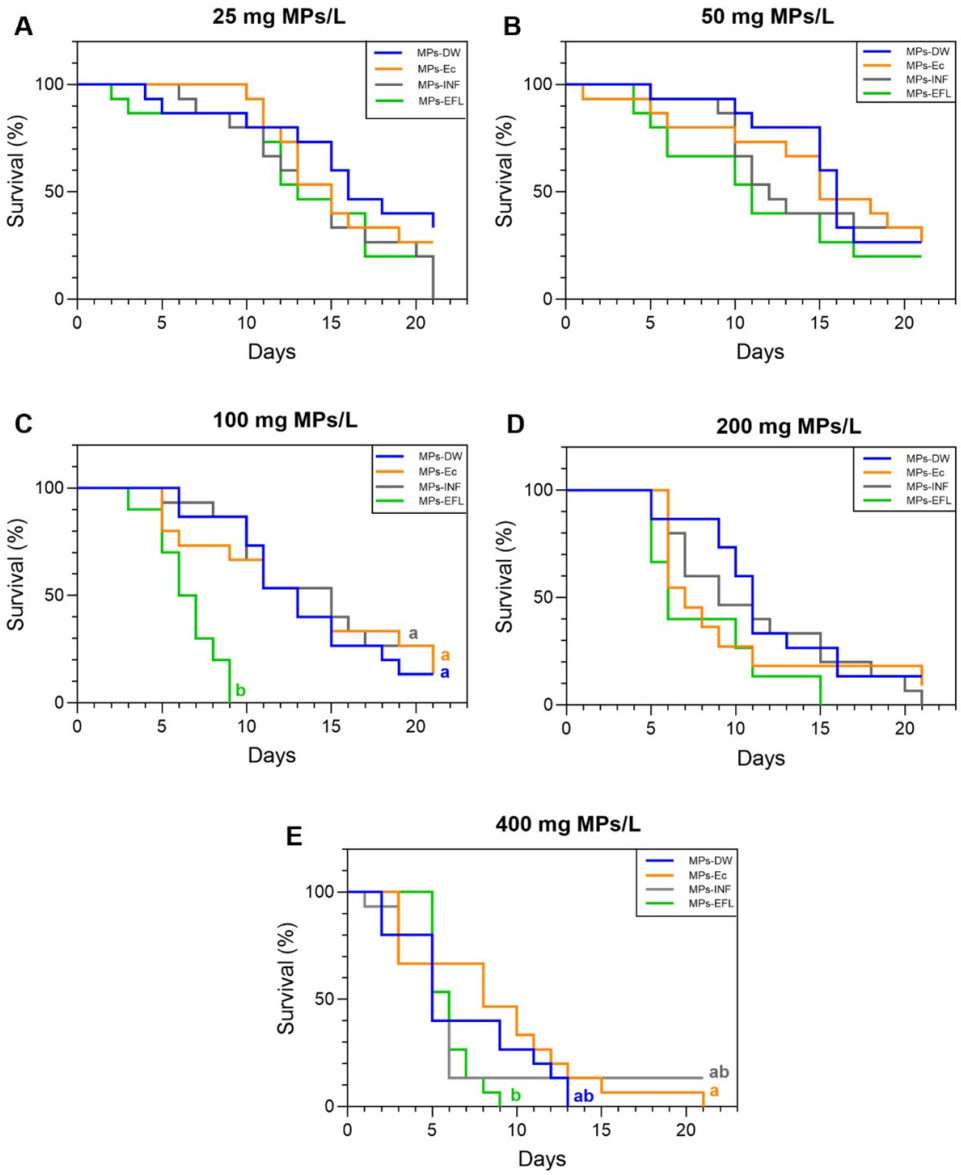

Figure S8: *Results of the Kaplan-Meier survival analysis for D. magna exposed for 21 days to concentrations of 0 (non-exposed control), 25 (A), 50 (B), 100 (C), 200 (D) and 400 (E) mg/L of MPs-DW, MPs-Ec, MPs-INF, MPs-EFL. The letters that appear to the right of each graph indicate if there are significant differences (p <0.05) or not between samples (different or same letter, respectively).*

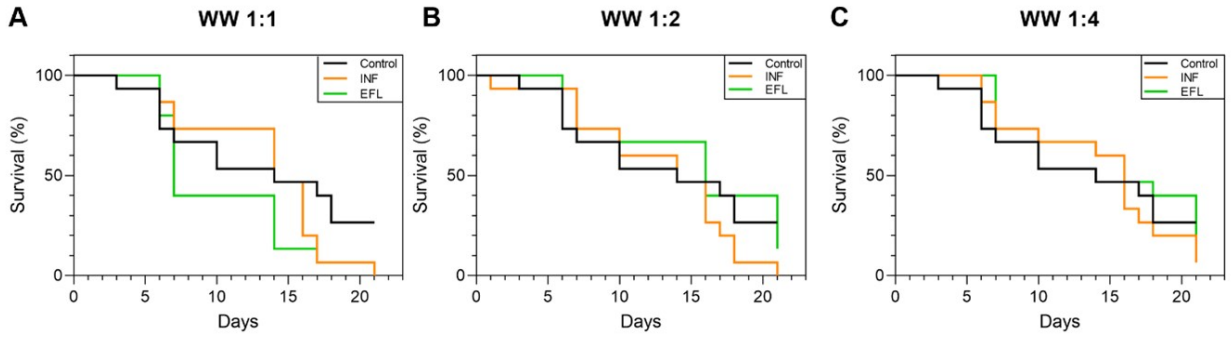

Figure S9: *Results of the Kaplan-Meier survival analysis for D. magna exposed for 21 days to concentrations of 1:1 (A), 1:2 (B), 1:4 (C) of wastewater from Influent (INF) and Efluent (EFL).*

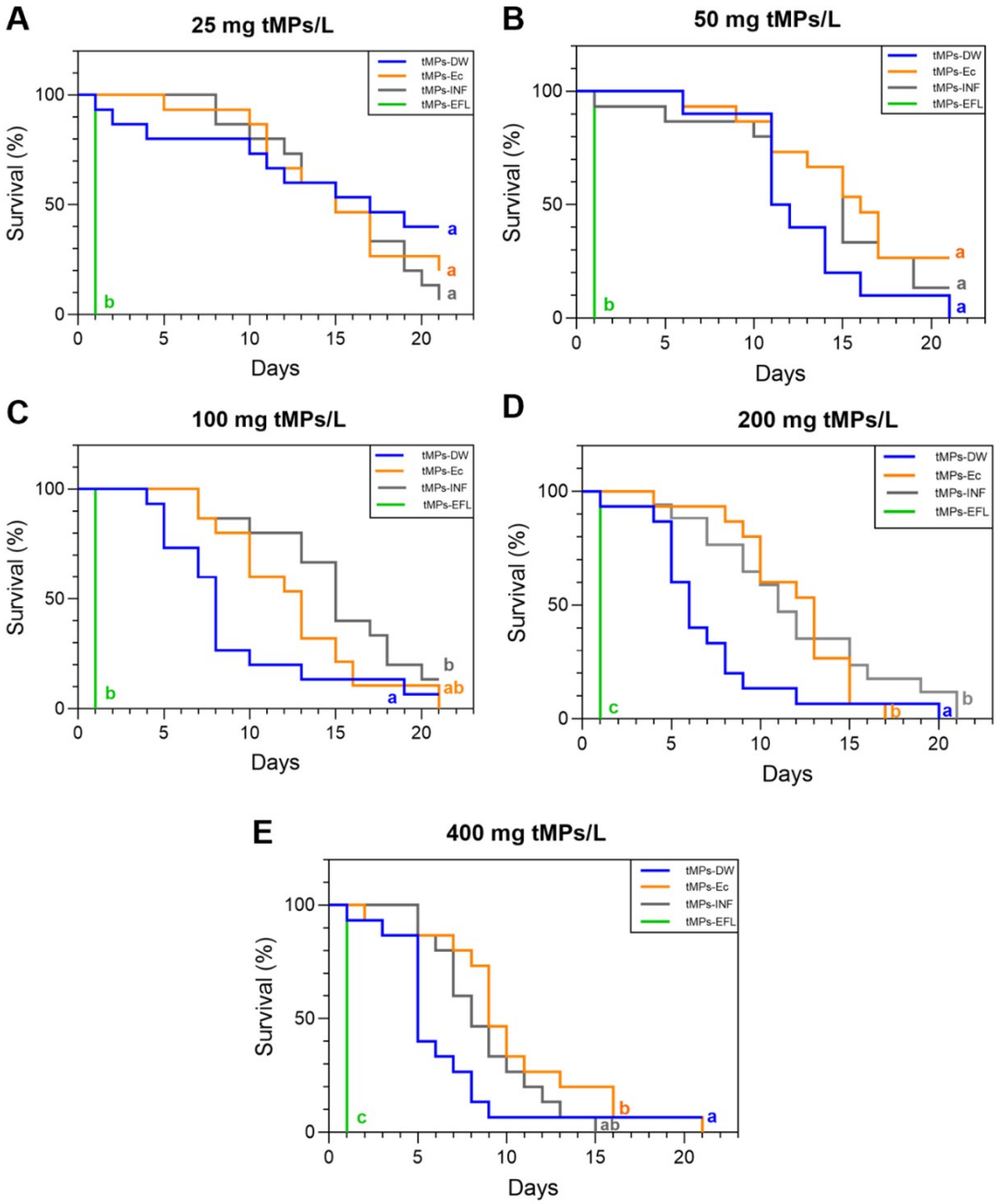

Figure S10: *Results of the Kaplan-Meier survival analysis for D. magna exposed for 21 days to concentrations of 25 (A), 50 (B), 100 (C), 200 (D), and 400 (E) mg/L of tMPs-DW, tMPs-Ec, tMPs-INF, MPs-tEFL . The letters that appear to the right of each graph indicate if there are significant differences (p <0.05) or not between samples (different or same letter, respectively).*